Food Chemistry 365 (2021) 130528

Contents lists available at ScienceDirect

Food Chemistry

journal homepage: www.elsevier.com/locate/foodchem

Gastrointestinal metabolism of monomeric and polymeric polyphenols from mango (*Mangifera indica* L.) bagasse under simulated conditions

Luz Abril Herrera-Cazares [a,1], Aurea K. Ramírez-Jiménez [b,1], Ivan Luzardo-Ocampo [a], Marilena Antunes-Ricardo [b], Guadalupe Loarca-Piña [a], Abraham Wall-Medrano [c], Marcela Gaytán-Martínez [a,*]

[a] Research and Graduate Program in Food Science, School of Chemistry, Universidad Autónoma de Querétaro, Cerro de las Campanas S/N. Col. Centro, 76010 Santiago de Querétaro, Qro., Mexico
[b] Tecnologico de Monterrey, School of Engineering and Science, Av. Eugenio Garza Sada 2501 Sur, C.P. 64849, Monterrey, N.L., Mexico
[c] Instituto de Ciencias Biomédicas, Universidad Autónoma de Ciudad Juárez, Anillo Envolvente del PRONAF y Estocolmo s/n, 32310 Ciudad Juárez, Chihuahua, Mexico

ARTICLE INFO

Keywords:
Mango (*Mangifera indica* L.) bagasse
Bioaccessibility
Principal component analysis
Simulated gastrointestinal digestion

Chemical compounds used in this article:
ABTS (PubChem CID: 9570474)
Acetonitrile (PubChem CID: 6342)
DPPH (PubChem CID: 74358)
Ethyl acetate (PubChem CID: 8857)
Formic acid (PubChem CID: 284)
Hexane (PubChem CID: 8058)
Methanol (PubChem CID: 997)
Pentobarbital sodium (PubChem CID: 23676152)
Sodium hydroxide (PubChem CID: 14798)

ABSTRACT

Mango bagasse (MB) is an agro-industrial by-product rich in bioactive polyphenols with potential application as a functional ingredient. This study aimed to delineate the metabolic fate of monomeric/polymeric MB polyphenols subjected to simulated gastrointestinal digestion. The main identified compounds by LC/MS-TOF-ESI were phenolic acids [gallic acid (GA) and derivates, and chlorogenic acid], gallotannins and derivatives [di-GA (DA) and 3GG-to-8GG], benzophenones [galloylated maclurins (MGH, MDH)], flavonoids [Quercetin (Quer) and (QuerH)] and xanthones [mangiferin isomers]. The bioaccessibility depended on the polyphenols' structure, being Quer, 5G to 8G the main drivers. The results suggested that the gastrointestinal fate of MB polyphenols is mainly governed by benzophenones and gallotannins degalloylation and spontaneous xanthone isomerization *in vitro* to sustain GA bioaccessibility.

1. Introduction

Mango (*Mangifera indica* L.) is probably the most important tropical fruit crop worldwide; its production reached ~ 38 million tons in 2017, primarily cultivated in Asia (74.4%), Africa (13.1%), and Latin America (12.4%). The industrial processing of mango into juice, nectar purée, ice cream, jam, canned slices, chutneys and, dry powders generates a considerable amount of by-products (35–60% w/w), including bagasse (MB), peels and, seeds (Wall-Medrano et al., 2020; Alañón et al., 2019).

MB has been defined as the seed and peel-free, remnant fiber-rich product after the juice extraction from the mango pulp (Wall-Medrano et al., 2020). Previous studies have shown that MB is a rich source of health-promoting bioactives (Anaya-Loyola et al., 2020; Herrera-Cazares et al., 2017; 2019;; Ramírez-Maganda et al., 2015). It is

Abbreviations: **3G**, Trigalloyl hexoside; **5G**, Pentagalloyl hexoside; **6G**, Hexa-*O*-galloyl hexoside; **7G**, Hepta-*O*-galloyl hexoside; **8G**, Octa-*O*-galloyl hexoside; **ABTS**, 2,2-azino-bis(3-ethylbenzothiazoline-6-sulfonic) acid; **AIF**, Absorbable intestinal fraction; **BIF**, Bioaccessible intestinal fraction; **CA**, Chlorogenic acid; **CIOMS**, Council for International Organizations of Medical Sciences; **DA**, Digallic acid; **DPPH**, 2,2-diphenyl-1-picrylhydrazyl; **ER**, Efflux ratio; **GA**, Gallic acid; **GH**, Galloyl hexoside; **HPLC-DAD**, High-performance liquid chromatography coupled to diode array detector; **LC/MS-TOF-ESI**, Liquid chromatography coupled to mass spectrometry with a time of flight and electrospray ionization; **Man**, Mangiferin; **MB**, Mango bagasse; **MDH**, Maclurin di-*O*-galloyl-hexoside; **MG**, Methyl gallate; **MGE**, Methyl gallate ester; **MGH**, Maclurin mono-*O*-galloyl-hexoside; **P_{app}**, Apparent permeability coefficient; **P_{app}A to B**, Apical to basolateral P_{app}; **P_{app}B to A**, Basolateral to apical P_{app}; **PCA**, Principal component analysis; **QuerH**, Quercetin-3-*O*-hexoside; **SGD**, Simulated gastrointestinal digestion.

* Corresponding author.
E-mail address: marcelagaytanm@yahoo.com.mx (M. Gaytán-Martínez).
[1] These authors equally contributed to this manuscript.

https://doi.org/10.1016/j.foodchem.2021.130528
Received 14 August 2020; Received in revised form 30 May 2021; Accepted 1 July 2021
Available online 5 July 2021

particularly rich in dietary fiber and polyphenols, with many health benefits associated with its antioxidant capacity and epigenetic action (Wall-Medrano et al., 2020). MB polyphenols and dietary fiber are also fermentable substrates that contribute to the production of many microbial metabolites under simulated colonic conditions, such as acetate, propionate, and butyrate and their acylated (C1-C4) and phenolic derivates, di-methyl-trisulfide, 1,3-di-*tert*-butyl-benzene, and several flavonoid derivates such as gallocatechin (Herrera-Cazares et al., 2019; Hernández-Maldonado et al., 2019).

MB has been used as a cereal flour replacer to reduce the fat content and oil-binding capacity while increasing the antioxidant capacity and phenolic profile of baked products. Such substitution also improves the nutritional profile of baked goods by adding protein, iron, potassium, and dietary fiber (Hernández-Maldonado et al., 2019; Ramírez-Maganda et al., 2015). Most of these properties have been partially validated through bioaccessibility and bioavailability studies from the mango by-products. For example, Herrera-Cazares et al. (2017) reported that the inclusion of MB for the manufacturing of functional confections contributed to a higher abundance and bioaccessibility of mangiferin (Man), gallic acid (GA), and quercetin (Que), providing higher antioxidant capacity than similar in-market goods. Polyphenols from mango by-products snacks (peel, seed, and paste-based snacks) showed the highest bioaccessibility at the gastric stage, while gallic acid and mangiferin were the main identified polyphenols (Bertha et al., 2019). The supplementation of corn chips with mango "Ataulfo" peel improved their phenolic content, significantly increasing the bioaccessible and dialyzable phenolic content (Zepeda-Ruiz et al., 2020). However, complete identification of the several polyphenol classes from MB has not been conducted, nor their metabolic fate along with digestion. This is critical since the extent to which a particular polyphenol is digested before reaching systemic translocation (first-pass metabolism) may also impact its potential health effects (Reis et al., 2020; Agudelo, Luzardo-Ocampo, Campos-Vega, Loarca-Pina, Maldonado-Celis et al., 2018). Therefore, this study aimed to evaluate the gastrointestinal metabolism of MB (*Mangifera indica* L.) polyphenols using a simulated gastrointestinal digestion (SGD) using two high-throughput chromatographic platforms (HPLC-DAD and LC/ESI-TOF-MS) and chemometric tools [principal component analysis (PCA)] to track molecular modifications and diversity.

2. Materials and methods

2.1. Materials

MB (*Mangifera indica* L. cv. Ataulfo) was provided by *Frozen Pulps de México S.A. de C.V.* The bagasse was extracted from mangoes at the R4 ripening state according to the classification system proposed by Cheema & Sommerhalter (2015), in which the mangoes are mature and slightly soft to the touch but present increasing yellow coloration. This particular ripening state was chosen since the commercial manufacturer of mango juice requires ripe mangoes at this state to obtain the juice. For obtaining the bagasse, the fruit is scalded at 92 °C for 15 min, cooled using cold water, and then peel and seeds are eliminated. The pulp is then extracted, and the remaining by-product is considered a peel-free MB. The resulting MB was frozen at −18° C, freeze-dried for 24 h, micronized (250 μm), and vacuum-stored at −70° C until use. The physicochemical characterization of the bagasse reporting the color measurement using the CIEL*a*b space parameters, the water absorption, and the water solubility indexes is included in **Supplementary Table S1A.** In addition, the physicochemical characterization of the original mango pulp used for the extraction of the bagasse is presented in **Supplementary Table S1B.**

2.2. Simulated gastrointestinal digestion (SGD)

The SGD was carried out as described previously (Campos-Vega et al., 2015) with slight modifications (Herrera-Cazares et al., 2017). This procedure was conducted to consider the impact of the physiological conditions on the potential release (bioaccessibility) of targeted phenolic compounds, defining the extent to which those compounds can potentially exert health benefits (Luzardo-Ocampo et al., 2020). Briefly, four healthy volunteers fasted for at least 90 min participated in the oral phase chewing the sample (1 g) 15 times for 15 s and expectorated it in a flask containing 5 mL of distilled water. The gastric conditions were simulated using pH-adjusted (2.0) aliquots from the oral phase (10 mL) mixed with pepsin from porcine gastric mucosa (≥2500 units/mg protein, Sigma-Aldrich, St. Louis, MO, US) (0.055 g in 0.94 mL 20 mM HCl). Samples were incubated in an oscillating water bath (2 h, 37 °C, 80 cycles/min). For the intestinal stage, gastric samples (5 mL) were pH adjusted (7.2–7.4), placed in a test tube, and mixed with bovine bile and pancreatin (3 mg and 2.6 mg, dissolved in 5 mL of CO_2 gasified-Krebs-Ringer buffer at pH 6.8) at 37 °C. These tubes contained an everted rat gut sac.

To evaluate apparent permeability, we used the rat everted gut sac technique. Briefly, male Wistar rats (250–300 g body weight, n = 6 per experiment) were fasted overnight (16 h) with water *ad libitum,* anesthetized with pentobarbital sodium salt (60 mg/kg body weight), and euthanized with CO_2. The small intestine (jejunum) was exposed after a midline cut, rinsed with Krebs-Ringer buffer (37 °C), and carefully cut (6 cm pieces) and everted. Sacs were then filled with Krebs-Ringer buffer, tied at both ends, and placed in the intestinal solution-containing tubes and incubated (37 °C for 15, 30, 60, and 120 min). After the incubation, the solution inside the sacs was considered the absorbable intestinal fraction (AIF), while the content outside of the gut sac was titled: bioaccessible intestinal fraction (BIF). Epithelial integrity and viability were ensured by assessing the rate of water absorption and efflux, as recently described (Luzardo-Ocampo et al., 2020). A diagram of the AIF and BIF fractions is shown in **Supplementary Fig. S1.**

This protocol was approved by the Bioethics Committee from the School of Chemistry of Universidad Autónoma de Querétaro (approval code: CBQ18/062) and followed the Guidelines for the Care and Use of Laboratory Animals from the National Institute of Health (NIH). As inclusion criteria for the healthy participants at the oral stage were considered the absence of dental apparatus, having all complete teeth, a normal weight (body mass index: 18.5–24.9 kg/m^2), and not presenting gastrointestinal problems in the last three months. Moreover, according to the *Helsinki Declaration* and the *Council for International Organizations of Medical Sciences* (CIOMS), the participants provided signed consent before they participated in the study. A pooled-saliva sample from all donors with no added sample was used as blank. Samples were stored at −70 °C for further analysis.

2.3. MB polyphenols extraction and identification

Both free and bound phenolics were extracted and characterized as follows. It is important to note that the characterization of bound polyphenols was carried out to fully characterize the initial polyphenolic composition of MB rather than conduct its characterization throughout digestion.

2.3.1. Extraction of free and bound polyphenols from MB

Free polyphenols were extracted from 1 g of the sample (MB) blended with 10 mL of ethanol/water solution (80:20 v/v) for 10 min in an orbital shaker (250 rpm). The samples were then centrifuged (3000*g*, 10 min at 4 °C), and supernatants were concentrated (Genevac, SP Scientific, Warminster, Pennsylvania, US) at 45 °C for 5 h. This extract was stored protected from light at −20 °C for further analyses.

The resulting precipitate was used to extract bound polyphenols. Nitrogen (N_2) was used for oxygen removal, and the sample was resuspended and stirred (250 rpm) in 10 mL NaOH (2 M) for 60 min at 25 °C. After a 30 min acid hydrolysis at 85 °C (HCl 12 M) under constant stirring (100 rpm), hexane (10 mL) was added. The acid-treated samples

were centrifuged at a speed of 1677*xg* for 10 min at 4 °C to eliminate the upper layer (hexane phase). Then, samples were washed with 10 mL ethyl acetate and centrifuged at 1677*g*, 10 min, 4 °C. The supernatant was recovered and concentrated (Genevac, SP Scientific, US) at 45 °C for 5 h. This residue was resuspended in 1 mL methanol and stored at −20 °C, protected from light for further analysis.

2.3.2. HPLC-DAD and LC/MS-TOF-ESI identification and quantification of MB polyphenols

Identification and quantification of selected polyphenols from the free and bound polyphenol extracts (undigested MB) and samples from all SGD stages were conducted as reported by Pacheco-Ordaz, Antunes-Ricardo, Gutiérrez-Uribe, & González-Aguilar (2018), with slight modifications. Quantification was performed in a high-performance liquid chromatography system coupled to a diode array detector (HPLC-DAD) (1300 Series, Agilent Technologies, Santa Clara, CA, US). Separation of polyphenols was performed in a Zorbax SB-AQ C18 column (3.0 × 150 mm, 3.2 mm) at 40 °C and flux gradient of 0.6 mL/min. The mobile phase was composed of two solvents: A: water/formic acid (0.1% formic acid) and B: acetonitrile/formic acid (0.1% formic acid). The gradient was established in isocratic gradients as follows: 5–20% B for 15 min and 20–100% B for 24 min. Chromatograms were generated at 280, 320, and 365 nm with an injection volume of 5 mL, and results were quantified as μg of gallic acid equivalents for phenolic acids, gallotannins and derivatives, and benzophenones; mangiferin equivalents for total xanthones, or (+)-quercetin equivalents for total flavonoids, per gram of sample, respectively.

The molecular identification was performed using liquid chromatography coupled to mass spectrometry with a time of flight and electrospray ionization platform (LC/MS-TOF-ESI) in an Agilent LCMS SQ 6120 system (Agilent-Technologies) equipped with a quaternary pump and automated vacuum degasser. Nitrogen was used as a gas carrier (350 °C, 10 L/min) and ion mass spectra were obtained in the negative mode ($[M-H]^-$, *m/z*) 140–1500 *m/z* range (fragmentation voltage: 50 V, gas temperature: 300 °C, misting: 40 psi, capillary voltage: 4000 V), and error mass cut-off of 1.5 ppm. The identification of compounds was conducted comparing the exact mass of the identified ions with the dictionary of natural products (http://dnp.chemnerbase.com) and confirmed with previous reports on mango polyphenols (Vazquez-Olivo et al., 2019; Dars et al., 2019; Pacheco-Ordaz et al., 2018; Jhaumeer Laulloo et al., 2018; Dorta et al., 2014; Sáyago-Ayerdi et al., 2013; Clifford et al., 2003). Their fragmentation pattern was also analyzed (**Supplementary Fig. S2**).

2.4. Bioaccessibility

The bioaccessibility of phenolic acids, gallotannins and derivatives, benzophenones, and xanthones from the *in vitro* digestion was done using the equation: B(%):[(C_f/C_0] * 100%, considering B as bioaccessibility (%), C_f is the final concentration of the compound at a selected stage or incubation time, and C_0 is the total amount of compounds of the same sample. These bioaccessibility values were used to express each group of compounds as a proportion (%) from the total composition at each SGD stage. The bioaccessibility of flavonoids was not included as only quercetin hexoside was detected during the digestion (**Supplementary Table S2**).

2.5. Ex vivo apparent permeability

Apparent permeability coefficients (*Papp*) for each identified compound in both directions [Apical (A) to basolateral (B) and B to A] were calculated with equation (1) (Lassoued, Khemiss, & Sfar, 2011):

$$P_{app}: \ (dQ/dt)/(1/A*C_0) \quad (1)$$

where dQ/dt (mg/s) is the amount of polyphenol transported through the sac per second, A is the permeation area (cm^2), and C_0 (mg/mL) is the initial concentration of the selected polyphenol before the intestinal incubation (gastric phase). Apical to basolateral (P_{app} A to B), basolateral to apical side (P_{app} B to A), their difference (P_{app} Net), and efflux ratio coefficient (ER= (P_{app} B to A/ P_{app} A to B), were further calculated.

2.6. Antioxidant capacity

The antioxidant capacity of bioaccessible polyphenols was tracked along the SGD by measuring radical scavenging capacity toward 2,2-azino-bis(3-ethylbenzothiazoline-6-sulfonic) acid (ABTS; 540 nm) and 2,2-diphenyl-1-picrylhydrazyl (DPPH; 734 nm) by previously standardized methods (Herrera-Cazares et al., 2017). A Trolox calibration curve (50–800 mM) was used, and results were expressed as micrograms of Trolox equivalents per mL of sample (μg TE/mL).

2.7. Statistical analysis

Unless otherwise specified, all analytical results were expressed as average values ± standard deviation (SD), from two independent experiments in triplicates. An analysis of variance (ANOVA) and *post-hoc* Tukey-Kramer's test was used to establish significant differences ($p < 0.05$). The best equation explaining the time-trend (15–120 min) changes in P_{app} (for a given polyphenol, assayed in the *ex vivo* apparent permeability assay, was further generated by regression analysis, maximizing R^2 values by the goodness-of-fit method. The JMP v. 14.0.0 software (SAS Institute Inc., Cary, NC) was used for all statistical analysis.

3. Results and discussion

3.1. Molecular identification and quantification of undigested MB polyphenols

Table 1, **Supplementary Table S2**, and **Supplementary Table S3** show the LC/MS-TOF-ESI tentative identification and quantification by HPLC-DAD of the primary polyphenols present in the undigested MB sample, as free and bound forms. Classification of these compounds was based on their structural similarity and molecular weight. The main identified compounds were four hydroxybenzoic acids [gallic acid (GA), methyl gallate (MG), methyl gallate ester (MGE), galloyl hexoside (GH)], one hydroxycinnamic acid [chlorogenic acid, CA)], and two benzophenones [Maclurin mono- (MGG) or di-*O*-galloyl hexoside (MDG)]. These xanthones share biosynthetic pathways with the three identified xanthones [mangiferin (Man), isomangiferin (IMan), and homomangiferin (HMan)]. Two flavonoids [quercetin (Quer) and (QuerH)] were identified while other hexoside-galloylated complex polyphenols were found: tri- (3G), penta- (5G), hexa- (6G), hepta- (7G), and octa- (8G)-*O*-galloyl hexoside, and di-gallic acid (DA) which is cleavage product from ≥ 6G gallotannin derivatives. Other authors have identified all these polyphenols in by-products from several mango varieties, including "Ataulfo" variety (Anaya-Loyola et al., 2020; Clifford et al., 2003; Dars et al., 2019; Dorta et al., 2014; Jhaumeer Laulloo et al., 2018; Pacheco-Ordaz et al., 2018; Sáyago-Ayerdi et al., 2013; Vazquez-Olivo et al., 2019).

Since HMan and IMan were also found in the bound phenolics extract, it suggests a covalent association with complex carbohydrates in the food matrix (Wall-Medrano et al., 2020; Herrera-Cazares et al., 2017). Several flavonoids are commonly found in mangoes as glycosides (quercetin-3-*O*-hexoside or QuerH) more than aglycones (Alañón et al., 2019). MB showed a similar gallotannin profile to a recently reported mango juice by-product, but this later contained peel (Anaya-Loyola et al., 2020).

Lastly, the percental composition of all these polyphenols in undigested (free and bounded) and digested MB is depicted in Fig. 1. Higher molecular diversity was observed in unbounded phenolic acids

Table 1
LC/MS-TOF-ESI tentative identification of phenolic compounds.

Tentative assignment	Code	Formula	RT	λ_{max} (nm)	[M-H]$^-$ (*m/z*)	AM (g/mol)	Main fragments	Tentative assignment	Rel. Abundance (%)	Ref.
	Phenolic acids									
Chlorogenic acid	*CA*	$C_{16}H_{18}O_9$	1.145	231, 276	353.0649	353	391.0385, 226.9844, 193.0307, 191.0157, 158.9985	354.08	85.81	1
Gallic acid	*GA*	$C_7H_6O_5$	1.639	271	169.0122	169	112.9926, 191.0157, 205.0311, 283.0120, 339.0295, 319.0314, 375.0618, 439.0705, 547.1420	170.02	82.32	2
Methyl gallate	*MG*	$C_8H_8O_5$	4.036	275	183.0314	183	112.9926, 158.9985	184.04	85.59	3
Galloyl hexoside	*GH*	$C_{13}H_{16}O_{10}$	1.761	279	331.0656	331	137.0053, 158.9985, 227.9860, 226.9844, 297.0307	332.07	83.79	2
Methyl gallate ester	*MGE*	$C_{15}H_{12}O_9$	8.128	229, 279	335.0357	335	112.9936, 158.9985, 226.9844, 335.0357	336.05	90.75	4
	Benzophenones									
Maclurin mono-*O*-GH	*MGH*	$C_{26}H_{24}O_{15}$	3.261	230, 282	575.1025	575	112.9926, 158.9985, 226.9844	576.10	85.62	5
Maclurin di-*O*-GH	*MDH*	$C_{33}H_{28}O_{19}$	7.625	229, 279	727.1032	727	112.9926, 158.9985, 226.9844, 421.0732	728.11	93.75	6
	Xanthones									
Mangiferin	*Man*	$C_{19}H_{18}O_{11}$	6.100	240, 257316, 366	421.0735	421	112.9926, 158.9985, 226.9844	422.08	83.93	2
Isomangiferin	*IMan*	$C_{19}H_{18}O_{11}$	6.187	240, 259316,	421.0966	421	112.9926, 137.0188, 158.9985, 423.0961	422.08	72.65	2
Homomangiferin	*HMan*	$C_{20}H_{20}O_{11}$	6.460	367	435.0969	435	158.9985, 226.9844, 423.1903	436.10	74.21	6
	Gallotannins and derivatives									
Digallic acid	*DA*	$C_{14}H_{10}O_9$	3.821	228, 270	322.0406	321	112.9926, 158.9985, 226.9844, 321.0182	322.00	82.00	2
Trigalloyl hexoside	*3G*	$C_{27}H_{24}O_{18}$	4.531	228, 274	636.1148	635	465.0778, 312.0668, 169.0124	636.09	87.00	6
Penta-*O*-galloyl hexoside	*5G*	$C_{41}H_{32}O_{26}$	14.276	230, 280	939.0937	939	112.9926, 158.9985, 226.9844, 469.0512	940.10	82.65	4,7
Hexa-*O*- galloyl hexoside	*6G*	$C_{49}H_{38}O_{30}$	17.537	218, 281	1091.1019	1091	112.9926, 158.9985, 226.9844, 545.0550, 602.0449	1092.11	82.20	6
Hepta-*O*-gallolyl hexoside	*7G*	$C_{56}H_{42}O_{33}$	18.750	234, 280	621.0543	621	112.9926, 158.9985, 226.9844, 349.0532, 487.0499, 1243.0873	1244.12	91.47	7
Octa-*O*-gallolyl hexoside	*8G*	$C_{63}H_{47}O_{37}$	19.251	233, 278	697.0573	697	112.9926, 158.9985, 226.9844, 1395.0979	1396.12	92.38	7
	Flavonoids									
Quercetin	*Quer*	$C_{15}H_{10}O_7$	19.893	258, 271360	301.0302	301	158.9985, 195.0083, 226.9844, 300.9904, 335.0357, 393.0335, 787.0868	302.04	86.20	2
Quercetin-3-*O*-hexoside	*QuerH*	$C_{21}H_{19}O_{12}$	13.054	254, 356	464.1094	463	158.9985, 195.0083, 226.9844, 300.9904, 335.0357, 393.0335, 787.0868	464.09	87.43	4

The tentative identification was conducted analyzing both the retention time (RT) and the fragmentation pattern of each compound. Ion mass [M−H]$^-$, accurate mass (AM), references (Ref.): [1] Clifford et al. (2003), [2] Pacheco-Ordaz et al. (2018), [3] Vázquez-Olivo et al. (2019), [4] Dorta et al. (2014), [5] Dars et al. (2019), [6] Jhaumeer Laulloo et al. (2018), [7] Sayago-Ayerdi et al. (2013).

(Fig. 1**A**), gallotannins and derivatives (Fig. 1**B**), and benzophenones (Fig. 1**C**) but not xanthones (Fig. 1**D**). Our preceding study (Herrera-Cazares et al., 2017) reported a relatively higher quercetin, gallic acid, and mangiferin content in the methanolic extract of the same MB used in this report. However, this by-product was combined with additional ingredients from a functional confection, which could protect phenolics. Mangiferin and gallic acid have been reported as abundant phenolics in mango bagasse (Bertha, Alberto, Tovar, Sáyago-Ayerdi, & Zamora-Gasga, 2019, whereas hepta-galloyl-hexoside, penta-galloyl hexoside and tri-galloyl hexoside are the major gallotannins (Anaya-Loyola et al., 2020).

3.2. Bioaccessibility of MB polyphenols under simulated oral/gastric conditions

According to Fig. 1 and **Supplementary Table S2 and S3**, phenolic acids (gallic and chlorogenic acids), gallotannins (7G and 6G), benzophenones (MGH), xanthones (mangiferin), and QuerH were the most bioaccessible compounds from each polyphenol classes at the oral and gastric stages.

Many reports sustain the effective release of different monomeric polyphenols (e.g., phenolic acids and xanthones) from mango by-products under oral conditions (Wall-Medrano et al., 2020), and hydrolyzation and deglycosylation processes under acidic pH may also contribute to gallic and chlorogenic acids release (Burton-Freeman, Sandhu, & Edirisinghe, 2017). As for quercetin, its absence may be due to potential hydrophobic interactions with food components or low α-amylase activity (Lucas-González et al., 2018).

The release of gallic and digallic acids as major hydrolytic products from MB gallotannins and derivatives agrees with its reported weight-driven release and rendering from mango pulp (Sáyago-Ayerdi et al., 2013). These results were also confirmed by Barnes et al. (2016), which reported the presence of several gallotannin derivatives (4G to 12G compounds) after non-enzymatic hydrolysis, suggesting that physiological conditions such as those used in this research (neutral pH and anaerobic environment) are enough for the release of gallic and digallic acids.

3.3. Impact of MB polyphenols in the antioxidant capacity during in vitro digestion

According to Fig. 2, the ABTS scavenging capacity of free polyphenols from undigested MB was 14% higher than that observed for bound polyphenols, although this difference was not detected with the

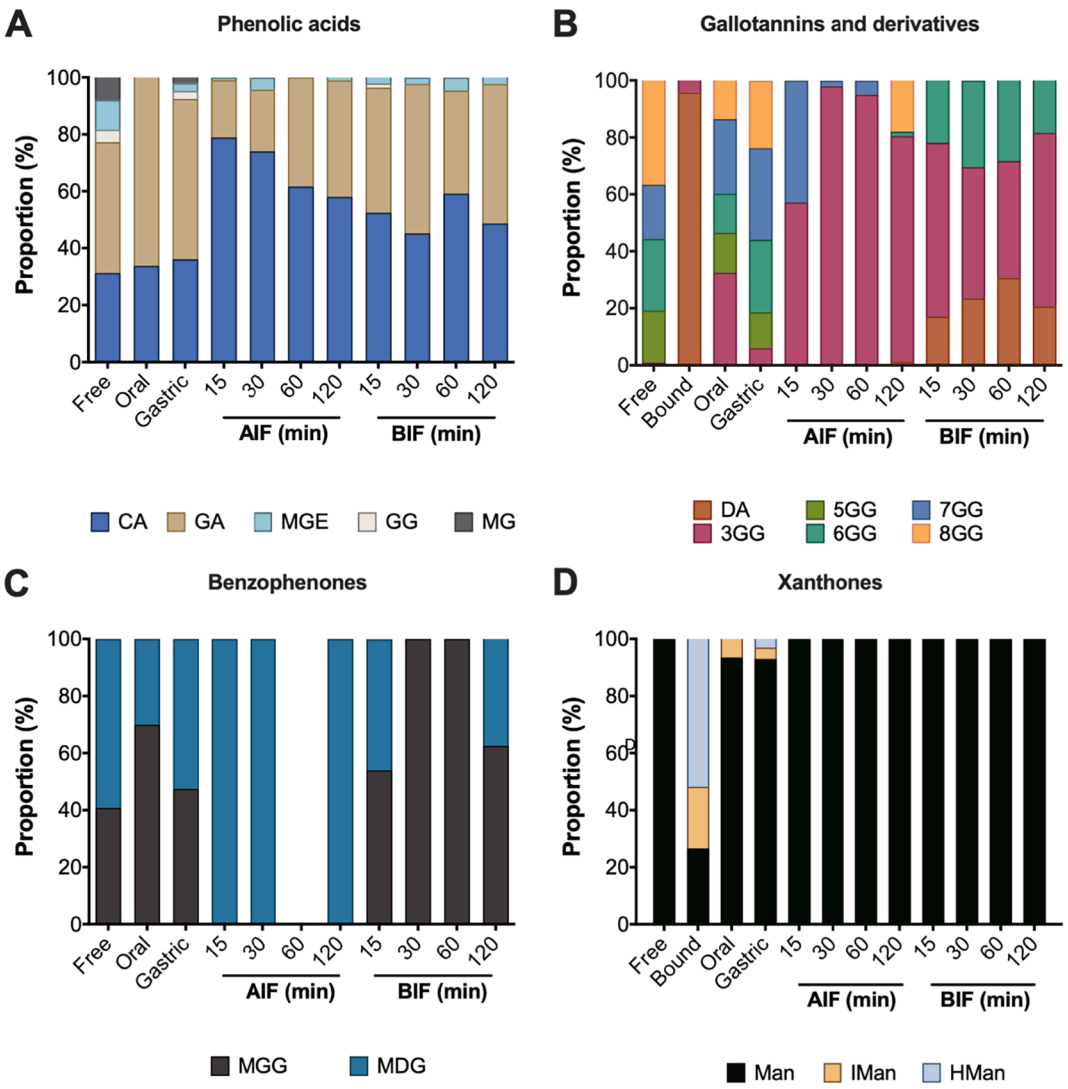

Fig. 1. Bioaccessibility of MB polyphenols during SGD. **(A)** Phenolic acids; **(B)** Gallotannins and derivatives; **(C)** Benzophenones; **(D)** Xanthones. The results were expressed as proportional composition (%) and are the results of bioaccessibility values from two independent experiments in triplicates. **3G:** Trigalloyl hexoside; **5G:** Pentagalloyl hexoside; **6G:** Hexa-*O*-galloyl hexoside; **7GG:** Hepta-*O*-galloyl hexoside; **8G:** Octa-*O*-galloyl hexoside; **AIF:** Absorbable intestinal fraction; **BIF:** Bioaccessible intestinal fraction; **CA:** Chlorogenic acid; **DA:** Digallic acid; **GA:** Gallic acid; **GH:** Galloyl hexoside; **HMan:** Homomangiferin; **IMan:** Isomangiferin; **Man:** Mangiferin; **MDH:** Maclurin di-*O*-galloyl-hexoside; **MG:** Methyl gallate; **MGE:** Methyl gallate ester; **MGH:** Maclurin mono-*O*-galloyl-hexoside; **SGD:** Simulated gastrointestinal digestion.

DPPH radical. As previously stated, the MB food matrix is rich in polymeric compounds, including dietary fiber and proteins to which MB polyphenols may be interacting (Herrera-Cazares et al., 2017; 2019). In a preceding study (Herrera-Cazares et al., 2017), we reported the same trend, yet lower values ($p < 0.05$) than those reported here, after correcting for different measurement units. This difference may be associated with different solvent extracting systems (EtOH: H2O vs. MetOH), freeze-drying processing, or a different MB lot.

Also, compared to undigested MB, the antioxidant capacity significantly dropped ($p < 0.05$) under simulated oral and gastric conditions (Fig. 2), a fact that could be associated with physiological conditions (dilution effect) and structural changes (macromolecular relaxation or new chemical bonding) during this passage. These results suggest that specific mechanisms of polyphenols digestion or their chemical structure might be affecting the antioxidant outcomes. For instance, flavonoids are more stable at low pH than phenolic acids. Other studies have correlated the amount of phenolic acids (e.g., coumaric and 2-hydroxybenzoic acids) in the BIF fraction of snacks made with mango by-products (peel, seed, and bagasse) with ABTS (Bertha, Alberto, Tovar, Sáyago-Ayerdi, & Zamora-Gasga, 2019). Moreover, gallic acid, methyl gallate, quercetin, and mangiferin from mango peel have been linked to high scavenging activity of ABTS and DPPH radicals due to their efficient activity as hydrogen donors from their easily-ionizable carboxylic group (Lizárraga-Velázquez, Hernández, González-Aguilar, & Heredia, 2018).

At the intestinal stage, a significant increase in the antioxidant capacity (ABTS method) was observed, a trend that has been reported in food matrices incorporating mango by-products (Bertha et al., 2019). It has been suggested that polyphenols interactions with dietary fiber or carbohydrate components (monosaccharides and oligosaccharides, among others), protect them from the digestive enzymes (Domínguez-Ávila et al., 2017). Moreover, the release of highly-permeable gallic acid suggests a contribution to the intestinal antioxidant capacity in the AIF fraction (Pacheco-Ordaz et al., 2018).

Lastly, the time-trend (15 to 120 min) antioxidant capacity observed for BIF was similar to AIF, particularly with the ABTS radical ($p < 0.05$) under simulated intestinal conditions, presumably due to a low absorption or a high transepithelial efflux.

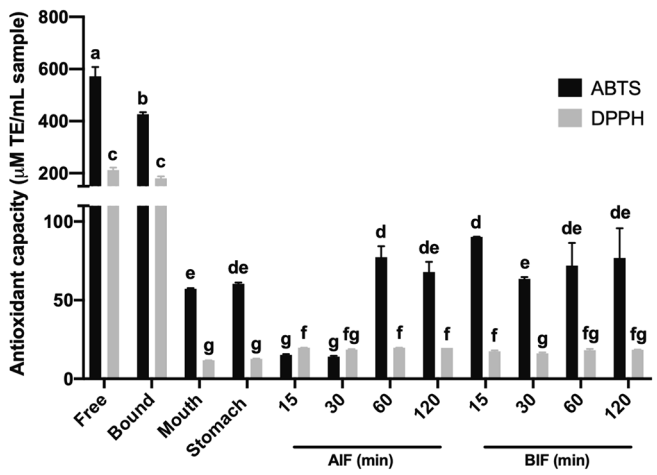

Fig. 2. Assessment of MB polyphenols in the antioxidant capacity during SGD. The results were expressed as the mean ± SD of three independent experiments, in triplicates. Different letters express significant differences ($p < 0.05$) by Tukey-Kramer's test. **AIF:** Absorbable intestinal fraction; **BIF:** Bioaccessible intestinal fraction; **SGD:** Simulated gastrointestinal digestion; **TE:** Trolox equivalents.

3.4. Intestinal bioaccessibility and apparent intestinal permeability of MB polyphenols

The *in vitro* digestion + *ex vivo* permeability (gut everted sac technique) biosystem used in this study closely mimic *in vivo* gastrointestinal digestion and absorption conditions (Reis et al., 2020), allowing the measurement of bioaccessibility and permeability of selected compounds embedded in a food matrix (Dahlgren & Lennernäs, 2019). Bi-directional (A-to-B and B-to-A) P_{app} values gave partial information on the interaction of MB polyphenols with the intestinal epithelium, luminal, and MB matrix components. In contrast, P_{app} Net and ER values express the relationship between bi-directional P_{app} values, which can be associated with the most plausible transport mechanisms. Table 2 shows the time-trend P_{app} (A to B, B to A, and Net) and ER values for each MB polyphenol under simulated intestinal conditions, while **Supplementary Table S4** shows the best equation explaining their time-trend kinetics (A to B and B to A). Three polyphenol groups were identified according to their permeability behavior: dynamic permeants (chlorogenic acid, gallic acid, mangiferin, methyl gallate ester, quercetin hexoside), BIF prone (digallic acid, MGH, 6G), and AIF prone (3G, MDH, 7G). However, other polyphenols were not or negligible detected at this stage (methyl gallate, GH, 5G, 8G, isomangiferin, homomangiferin, and quercetin).

$P_{app\ A\ to\ B}$ and $P_{app\ Net}$ values 15 min after initiated the simulated intestinal stage for dynamic permeants were chlorogenic acid > QuerH > gallic acid, mangiferin, MGE, but their mean efflux ratio ($ER_{15\text{-}120\ min}$) was mangiferin > gallic acid > MGE > chlorogenic acid, QuerH. Gallic acid's and mangiferin's permeability behavior are in agreement with previous reports from other authors. For instance, $P_{app\ A\ to\ B}$ values of 1.5 and 2.5 × 10^{-6} cm/s has been reported for pure mangiferin and gallic acid at 120 min using a Caco-2/HT-29 cell monolayer system (Pacheco-Ordaz et al., 2018), whereas Jiamboonsri et al. (2015) showed $P_{app\ A\ to\ B}$ and $P_{app\ B\ to\ A}$ values of 1.0, 0.52 and 3.70 × 10^{-6} cm/s for the major polyphenols (gallic acid, MG, and 5G, respectively) of mango cv. "Fahlun" seed kernel in a Caco-2 monolayer system. Similarly, Vazquez-Olivo et al. (2019) reported $P_{app\ A\ to\ B}$ values from mango bark of three cultivars ("Keith", "Ataulfo", and "Tommy Atkins") for mangiferin and gallic acid ranging 1.8–7.5 × 10^{-5} cm/s.

Kinetic data (**Table S3**) also suggested that apical bioavailability of mangiferin, gallic acid, and chlorogenic acid is coupled to an efficient transport to the basolateral compartment with a polynomial [X^2 (A to B, $R^2 \geq 0.94$) and X^3 (B to A, $R^2 = 0.99$)] time-trend behavior, a fact previously observed in a preceding study (Herrera-Cazares et al., 2017). Interestingly, Andean berries (*Vaccinium meridionale* Swartz) are richer in chlorogenic acid and gallic acid than MB, yet their time-trend apparent permeability follows a similar X^2 ($P_{app\ A\text{-}to\text{-}B}$, $R^2 \geq 0.97$) and X^3 ($P_{app\ B\text{-}to\text{-}A}$, $R^2 = 0.99$) polynomial behavior (Agudelo et al., 2018). As the apparent permeability of all detected gallotannins was either AIF (3G, 7G) or BIF (6G) prone (Tables 2 and **Supplementary Table S3**). Data suggest that gallic acid's apical pool could be fulfilled with its free form within the first 30 min and with galloyl moieties derived from the hydrolysis of gallotannins afterward, as it will be further discussed.

It has been reported that 50% of all mango pulp (and so, MB) polyphenols are pro-gallic acid substrates, as shown by the trend of intestinal hydrolysis of 5G-7G gallotannins derivatives to increase the apical pool of 3G (30–120 min). As such, reports have shown the partial hydrolysis of 5G to 4G and 3G *in vitro* (Caco-2 cell monolayers) (Cai et al. 2006) and the spontaneous degalloylation of 6G-8G under simulated intestinal conditions (Krook & Hagerman, 2012). Regarding xanthones, isomangiferin and homomangiferin were isomerized back to mangiferin, potentially increasing the antioxidant capacity of samples and bioaccessibility since this latter compound has exhibited these properties (Domínguez-Ávila et al., 2017; Ehianeta et al., 2016). The presence of mangiferin at the gastric and intestinal stages has also been reported for mango based-snack bars, but lower contents were reported at the intestinal stage, probably due to intestinal enzymes (Hernández-Maldonado et al., 2019).

$P_{app\ A\ to\ B}$ and $P_{app\ B\ to\ A}$ values (Table 2) time-trend kinetic equations (**Supplementary Table S3**) for QuerH but mostly MGE are practically the same suggesting a gradient-dependent permeability. It has been reported that the glycosylation of polyphenols increases their chances to be transported along the intestinal barrier aimed by glucose transporters. Several authors have pointed out that glycosylation of polyphenols increases the odd for absorption since several glucose transporters join the already diverse A-to-B and B-to-A active transport alternatives for these aglycones (Domínguez-Ávila et al., 2017). The abundance of MGE could be linked to the potential chemical transformation of galloyl metabolites (4-*O*-methyl gallic and 4-*O*-methyl gallic acid-3-*O*-sulfate) that has been detected in human plasma after mango "Ataulfo" pulp consumption (Barnes et al., 2019).

Some other MB polyphenols were partially constrained in the apical (3G > MDH > 7G) and basolateral (MGH > digallic acid, 6G) sides (**Supplementary Table S3**). MDH was the third most bioaccessible polyphenol (along with chlorogenic and gallic acids) in the first 15 min after initiated the intestinal stage; this phenomenon led to the highest $P_{app\ B\text{-}to\text{-}A}$ (54.6 ± 3.7 cm/s × 10^{-5}) and $P_{app\ Net}$ (48.8 ± 3.4 cm/s × 10^{-5}) values (Table 2) and the most erratic X^3-polynomial behavior of all MB polyphenols (**Table S2**). Interestingly, if we considered that most MGH coming from the gastric stage (27 mg GAE/g, **Supplementary Table S3**) rapidly crossed the gut epithelia in the A-to-B direction (20 mg GAE/g), an additional basolateral accumulation of MGH from 30 to 120 min seemed to be related to a time-trend reduction of MDH in the apical side (between 15 and 120 min). As for digallic acid and 3G, 6G, and 5G, their transepithelial movement (**Supplementary Table S2 and S3**) and ultimate kinetics (**Supplementary Table S4**) seem to be related to the stepwise de-galloylation previously commented (Barnes et al., 2019, Krook & Hagerman, 2012, Cai et al., 2006).

3.5. Principal components analysis (PCA)

According to Fig. 3 and **Supplementary Fig. S3**, PC1 (44.5%), PC2 (18.7%), and PC3 (12.5%) explained 81% of the total variance, and the most influencing variables were galloyl hexoside, methyl gallate, MGE, and 5G-to-8G (PC1, eigenvalues from 0.28 to 0.31), gallic acid, MGH, digallic acid, mangiferin, DPPH, ABTS (PC2, eigenvalues from −0.36 to −0.33 and 0.25 to 0.32) and CA, MGE, MDH, homomangiferin, digallic acid, MGH (PC3, eigenvalues from −0.42 to −0.21 and 0.47 to 0.23),

Table 2
Apparent permeability (P_{app}) and efflux ratios (ER) for mango bagasse-derived polyphenols under *ex vivo* intestinal conditions[1].

Dynamic permeants					
CA	15	16.4 ± 3.1 ^{a}	33.0 ± 0.8 ^{a}	16.2 ± 3.5^{b}	0.5 ± 0.1^{b}
	30	7.1 ± 2.2 ^{a}	2.2 ± 0.2^{b}	5.0 ± 2.4 ^{a}	3.5 ± 1.3 ^{a}
	60	2.7 ± 0.6 ^{a}	2.6 ± 0.3^{b}	0.1 ± 0.9 ^{a}	1.1 ± 0.3 ^{ab}
	120	2.2 ± 0.1^{b}	1.7 ± 0.2^{b}	0.6 ± 0.2 ^{a}	1.4 ± 0.2 ^{ab}
GA	15	10.7 ± 1.8 ^{a}	5.7 ± 0.1 ^{a}	5.1 ± 1.7 ^{a}	1.9 ± 0.3^{b}
	30	5.4 ± 1.1^{b}	0.4 ± 0.1^{b}	4.9 ± 1.0 ^{ab}	12.3 ± 0.5 ^{a}
	60	1.7 ± 0.8^{b}	1.2 ± 0.3^{b}	0.5 ± 1.0 ^{ab}	2.2 ± 1.5^{b}
	120	1.5 ± 0.1^{b}	0.8 ± 0.2^{b}	0.7 ± 0.2^{b}	2.3 ± 0.8^{b}
MGE	15	9.4 ± 1.4 ^{a}	5.7 ± 1.00 ^{a}	3.7 ± 0.8 ^{a}	1.7 ± 0.2^{b}
	30	4.5 ± 0.3^{b}	1.7 ± 0.01 ^{a}	2.8 ± 0.4 ^{a}	2.6 ± 0.3 ^{ab}
	60	3.3 ± 1.4^{b}	–	3.3 ± 1.4 ^{a}	–
	120	1.4 ± 30.4^{b}	0.3 ± 0.1 ^{a}	1.0 ± 0.3 ^{a}	3.8 ± 0.4 ^{a}
Man	15	6.0 ± 1.9 ^{a}	1.0 ± 0.01 ^{a}	5.0 ± 1.9 ^{a}	6.3 ± 2.0 ^{ab}
	30	4.1 ± 0.6 ^{ab}	0.3 ± 0.01^{b}	3.7 ± 0.5 ^{ab}	13.1 ± 1.0 ^{a}
	60	1.2 ± 0.4^{b}	0.3 ± 0.01^{b}	0.9 ± 0.4 ^{ab}	4.6 ± 2.2^{b}
	120	0.8 ± 0.1^{b}	0.2 ± 0.01^{b}	0.6 ± 0.1^{b}	4.2 ± 1.0^{b}
QuerH	15	11.9 ± 1.2 ^{a}	5.9 ± 1.2 ^{a}	5.9 ± 0.3 ^{a}	2.1 ± 0.3 ^{a}
	30	4.2 ± 0.9^{b}	1.8 ± 0.4^{b}	2.4 ± 0.7^{b}	2.4 ± 0.3 ^{a}
	60	1.9 ± 0.5 ^{bc}	–	1.9 ± 0.5 ^{bc}	–
	120	0.6 ± 0.05^{c}	0.3 ± 0.04^{b}	3.0 ± 0.4^{c}	2.0 ± 0.3 ^{a}
Apical (A) prone					
MDH	15	5.8 ± 0.4 ^{a}	54.6 ± 3.7 ^{a}	48.8 ± 3.4^{b}	0.1 ± 0.0^{b}
	30	-	0.4 ± 0.1^{b}	0.4 ± 0.1 ^{a}	-
	60	-	-	-	-
	120	0.2 ± 0.1^{b}	0.3 ± 0.01^{b}	0.1 ± 0.0 ^{a}	0.8 ± 0.1 ^{a}
7G	15	–	0.2 ± 0.05 ^{a}	0.2 ± 0.05 ^{a}	–
	30	–	0.1 ± 0.01^{b}	0.1 ± 0.01^{b}	–
	60	–	0.1 ± 0.02 ^{ab}	0.1 ± 0.02^{b}	–
	120	–	0.2 ± 0.05 ^{a}	0.2 ± 0.05 ^{a}	–
3G	15	3.4 ± 0.6 ^{a}	1.5 ± 0.02 ^{d}	6.9 ± 0.8 ^{a}	5.8 ± 1.2 ^{a}
	30	2.7 ± 1.2^{b}	14.1 ± 1.1 ^{a}	11.4 ± 0.9^{c}	0.2 ± 0.1^{b}
	60	0.6 ± 0.1^{b}	9.5 ± 0.4^{b}	9.0 ± 0.4^{c}	0.1 ± 0.01^{b}
	120	0.8 ± 0.1^{b}	6.5 ± 0.5^{c}	5.7 ± 0.6^{b}	0.1 ± 0.02^{b}
DA	15	3.1 ± 0.02 ^{a}	-	3.1 ± 0.02 ^{a}	-
	30	0.2 ± 0.1 ^{ab}	-	0.2 ± 0.1 ^{ab}	-
	60	0.1 ± 0.0 ^{bc}	-	0.1 ± 0.0 ^{bc}	-
	120	0.1 ± 0.01^{c}	0.02 ± 0.01	0.02 ± 0.01^{c}	3.3 ± 1.0
MGG	15	8.1 ± 0.1 ^{a}	–	8.1 ± 0.1 ^{a}	–
	30	1.9 ± 1.2^{b}	–	1.9 ± 1.2^{b}	–
	60	0.6 ± 1.6^{b}	–	0.6 ± 1.6^{b}	–
	120	0.5 ± 0.1^{b}	–	0.5 ± 0.1^{b}	–
6G	15	0.5 ± 0.05 ^{a}	–	0.5 ± 0.05 ^{a}	–
	30	0.4 ± 0.08 ^{a}	–	0.4 ± 0.08 ^{a}	–
	60	0.1 ± 0.01^{b}	–	0.1 ± 0.01^{b}	–
	120	0.1 ± 0.01^{b}	0.03 ± 0.00	0.03 ± 0.01^{b}	1.9 ± 0.4

[1] Data is presented as mean ± SD of three independent experiments, P_{app} values are expressed as cm/s ($\times 10^{-5}$). See Table 1 for compound codes. Different letters within a same time-trend series (15–120 min) per compound and P_{app} value, means statistical differences ($p < 0.05$). –: Not detected.

respectively. Considering that MGE, digallic acid and, MGH influenced either PC1 or PC2, PC3 was not considered an important canonical variable. Among MB polyphenols, quercetin, 5G-8G, and methyl gallate (PC1) seemed to be responsible for the variance associated with the antioxidant activity (PC2, Fig. 3).

PCA also confirmed (by comparing the loading and score plots, Fig. 3) that CA ($BIF_{15,\ 120\ min}$ and oral) and gallic acid > MGH, mangiferin (gastric) were the most bioaccessible compounds and that all other MB polyphenols followed a stage-specific bioaccessibility. Lastly, the proximity of AIF (purple ellipse) and BIF (blue ellipse), particularly $AIF_{15\ min}$ (Fig. 3**B**) closed to $BIF_{30\ min}$, stands for a stepwise gradient-dependent transfer of MB polyphenols in the A-to-B direction. Similar SGD-stage discrimination patterns have also been found for polyphenols from durum-wheat fresh pasta (Rochetti et al. 2020) and grape juice sediments (da Silva et al., 2019).

3.6. Stepwise digestive metabolism of MB polyphenols

Fig. 4 resumes the proposed digestive metabolic pathways and bioaccessibility (%) changes for the most abundant MB polyphenols identified by LC-MS/TOF-ESI during the SGD used in this study. Herein we describe polyphenols' chemical catabolism for each of the digestive stages.

Oral stage. Although a higher diversity of polyphenols was found in the undigested MB (Fig. 4**A**), a remarkable reduction in polyphenol abundance was observed at this stage (Fig. 4, second segment): Free polyphenols coming from undigested MB were phenolic acids (gallic and chlorogenic acids), benzophenones (MDH and MGH), and mangiferin, but the amount of polymeric MB polyphenols (5G-8G) was negligible. However, bound polyphenols such as 3G (gallotannin derivatives) and isomangiferin were also detected. An increase in bioaccessibility (%) for certain compounds, such as gallic acid and mangiferin, suggests their release ability by mechanical effort (Dars et al., 2019; Herrera-Cazares et al., 2017; 2019;; Ramírez-Maganda et al., 2015). We also hypothesize that the higher gallic acid bioaccessibility along SGD stages is due to steady-state depolymerization (or hydrolysis) of gallotannins, digallic acid, and other monogalloylated polyphenols such as methyl gallate, MGE, MGH, and MDH (Kiss & Piwowarski, 2019). Although the residence time in the oral cavity may not be enough to release a substantial amount of polymeric polyphenols; nevertheless, MDH could be degalloylated to MGH at this stage. Lastly, isomangiferin bioaccessibility also had an important increase, which indicates a possible chemical

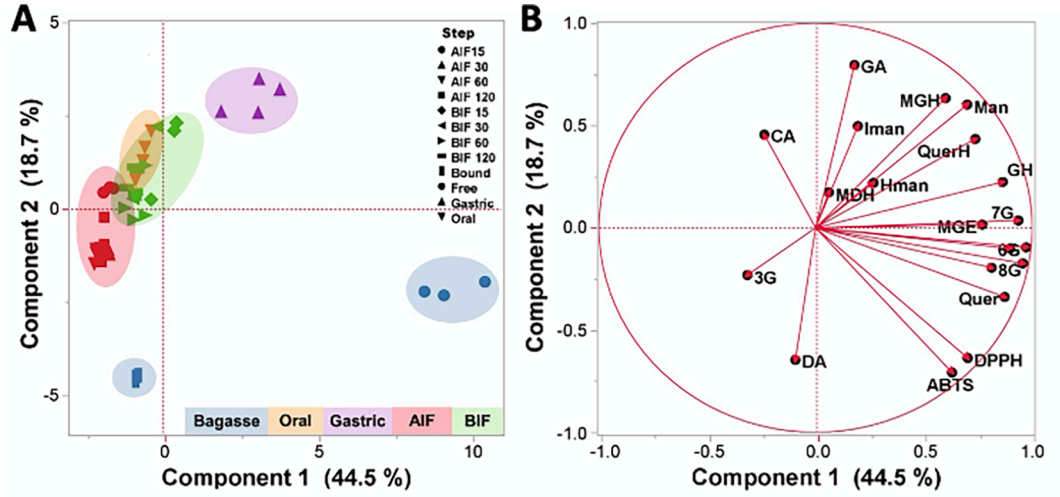

Fig. 3. Principal component analysis (PCA) of MB polyphenols and antioxidant capacity clustered by SGD stages. **(A)** Loading and **(B)** Scatter plots of the first and second component. **3G:** Trigalloyl hexoside; **5G:** Pentagalloyl hexoside; **6G:** Hexa-*O*-galloyl hexoside; **7G:** Hepta-*O*-galloyl hexoside; **8G:** Octa-*O*-galloyl hexoside; **AIF:** Absorbable intestinal fraction; **BIF:** Bioaccessible intestinal fraction; **CA:** Chlorogenic acid; **DA:** Digallic acid; **GA:** Gallic acid; **GH:** Galloyl hexoside; **HMan:** Homomangiferin; **Man:** Mangiferin; **MDH:** Maclurin di-*O*-galloyl-hexoside; **MG:** Methyl gallate; **MGE:** Methyl gallate ester; **MGH:** Maclurin mono-*O*-galloyl-hexoside; **Quer:** Quercetin; **QuerH:** Quercetin hexoside; **SGD:** Simulated gastrointestinal digestion.

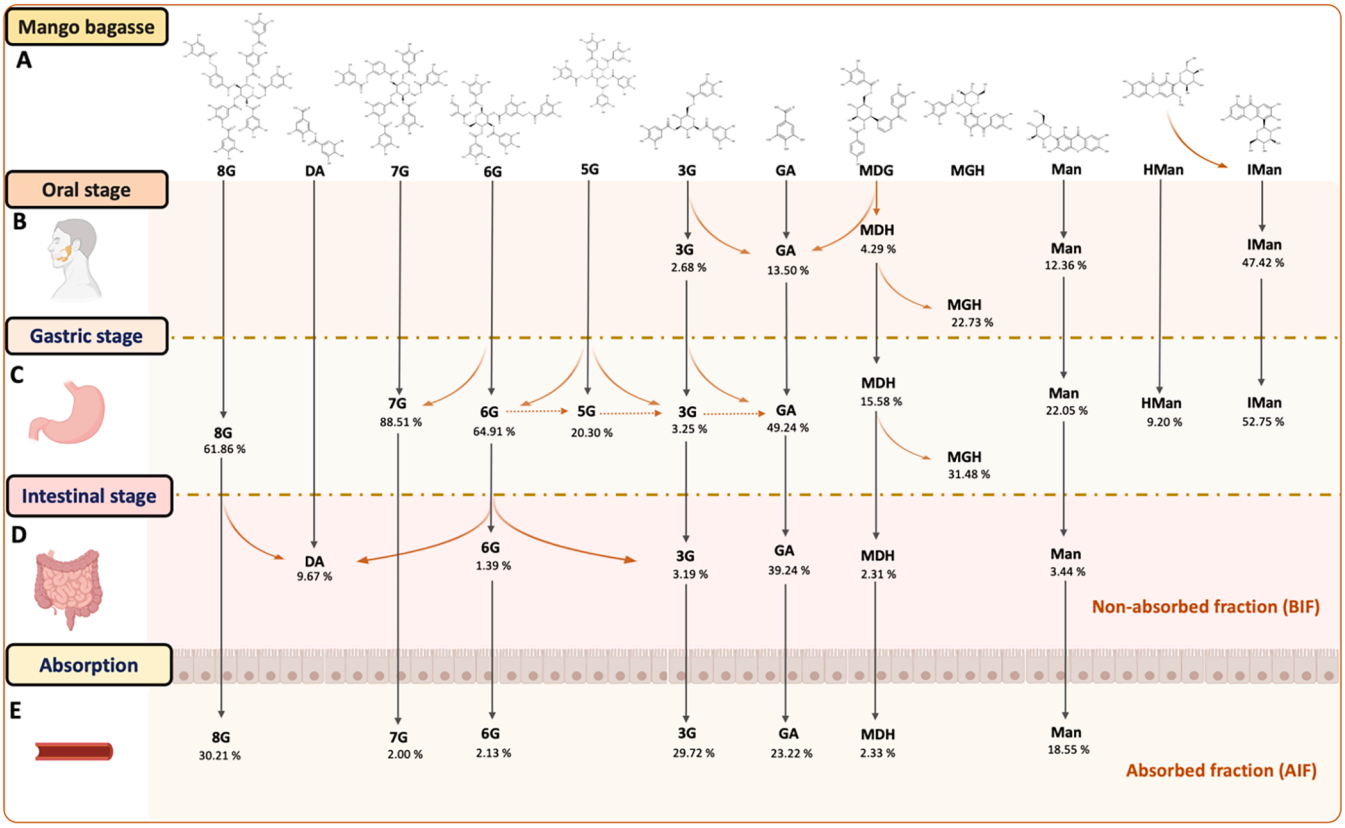

Fig. 4. Proposed digestive pathways of LC/MS-TOF-ESI identified MB polyphenols through the SGD stages. The letters indicate the stages: **(A)** Undigested MB; (**B**) Oral stage; (**C**) Gastric stage; (**D**) Small intestine stage. Dashed lines indicate the absence of the selected polyphenol at a certain stage. Lines or arrows for a certain compound of the same color indicates its passage through the digestion stages. Polyphenols inserted in the enterocyte section (border section between BIF and AIF) were detected in both stages. Percentages indicate the individual bioaccessibility of each compound at each *in vitro* digestion step. Bioaccessibility values at the intestinal stage refer to 120 min. Quercetin was not considered due to its low bioaccessibility at all stages. **3G:** Trigalloyl hexoside; **5G:** Pentagalloyl hexoside; **6G:** Hexa-*O*-galloyl hexoside; **7G:** Hepta-*O*-galloyl hexoside; **8G:** Octa-*O*-galloyl hexoside; **AIF:** Absorbable intestinal fraction; **BIF:** Bioaccessible intestinal fraction; **DA:** Digallic acid; **GA:** Gallic acid; **HMan:** Homomangiferin; **IMan:** Isomangiferin; **Man:** Mangiferin; **MDH:** Maclurin di-*O*-galloyl-hexoside; **MGH:** Maclurin mono-*O*-galloyl-hexoside; **SGD:** Simulated gastrointestinal digestion.

transformation from mangiferin and homomangiferin. Such isomeric interplay between these compounds was constant throughout the simulated gastrointestinal digestion stages.

Gastric. Macromolecular relaxation seems to be responsible for the highest bioaccessibility of MB polyphenols under low pH and pepsin action; such conditions may simultaneously cause the instability of polymeric polyphenols. As previously stated, gallic acid was one of the most abundant compounds at the intestinal step (bioaccessibility: 49.2%), partially due to a stepwise 8G → 7G → 6G (also digallic acid donors) → 5G, 3G depolymerization and a further release of gallic acid, and subsequently increasing its bioaccessibility. Such an event has also been observed *in vitro* (Kiss & Piwowarski, 2019). A more intense MDH degalloylation rendering MGG + free GA as by-products and isomangiferin, homomangiferin → mangiferin isomerization, occurred under gastric conditions, responsible for the increase of mangiferin bioaccessibility (up to 22.05%). It should be pointed out that other galloylated compounds (galloyl hexoside, MG, MGH) had little or no contribution to gallic acid's availability under gastric conditions (**Table S1**).

Intestinal. According to Pacheco-Ordaz et al. (2018), gallotannins can permeate Caco-2 cell monolayers due to specific transporters and then be degraded intracellularly to gallic and digallic acids. Conversely, Jiamboonsri et al. (2015) reported the ability of 5G and methyl gallate to potentially cross the epithelial barrier *in vitro* due to strong affinities found between these compounds and the membrane. However, they exhibit low absorptive transport due to their degree of hydroxylation and molecular configuration. The authors also observed *in vivo* the ability of 5G, methyl gallate, and gallic acid to be transported by the paracellular mechanism through the epithelial barrier, to be metabolized and accumulated in particular organs and tissues, and to be excreted in urine and feces, confirming both digestive and hepatic transformation.

Since gallotannins are digested to low-molecular-weight compounds (gallic and digallic acids) almost entirely as previously reported for higher-molecular weight gallotannins (decreasing its bioaccessibility to 30.21% and 2.0% for 8G and 7G, respectively) (Kiss & Piwowarski, 2019), their temporal residence in the BIF fraction may further allow their potential further biotransformation by gut microbiota to other compounds not tracked in this study (e.g., pyrogallol) with higher bioactivity (Bertha et al., 2019).

4. Conclusion

MB is a rich source of polyphenols that suffer biotransformation processes during digestion due to the physiological pH, temperature, and enzymatic activity. Significant contents of bioaccessible phenolic acids, gallotannins and derivatives, benzophenones, and xanthones were detected along with the digestion. The PCA analysis clustered selected polyphenols during the digestion stages, suggesting a central contribution of DA to antioxidant capacity. Biotransformation pathways validated a high abundance of phenolic acids at the undigested MB and the oral stage, degradation of gallotannins at the gastric and intestinal stage, and the relative stability of QuerH during the intestinal stage. Since meaningful reductions of certain polyphenols were observed, these results suggested the need to protect these compounds using suitable food matrices or food processing technologies to take advantage of MB composition and derived antioxidant capacity. However, considering that all of these results were obtained from bagasse extracted from mangoes in their commercial ripeness state (R4), more research is needed taking into account a higher diversity of ripeness.

CRediT authorship contribution statement

Luz Abril Herrera-Cazares: Data collection, data analysis, writing-original draft. **Aurea K. Ramirez-Jimenez:** Data analysis, writing-original draft, writing-review and editing. **Ivan Luzardo-Ocampo:** Data analysis, writing-original draft, writing-review and editing. **Marilena Antunes-Ricardo:** Data analysis, funding acquisition. **Guadalupe Loarca-Piña**: Data analysis, writing-review and editing. **Abraham Wall-Medrano:** Data analysis, writing-review and editing. **Marcela Gaytán-Martínez:** Conceived and designed the analysis, Data Analysis, Project administration, funding acquisition.

Declaration of Competing Interest

The authors declare that they have no known competing financial interests or personal relationships that could have appeared to influence the work reported in this paper.

Acknowledgments

Authors Luz Abril Herrera-Cazares and Ivan Luzardo-Ocampo acknowledges Consejo Nacional de Ciencia y Tecnología (CONACyT-Mexico) for their graduate studies scholarships [grant numbers: 855189 and 384201]. The valuable assistance of MVZ Martín García Servín (Instituto de Neurobiología, UNAM-Campus Juriquilla) providing the rats for the *in vitro* digestion, and M.Sc. Angel H. Cabrera-Ramírez for the conduction of the PCA analyses is also well appreciated. This project was funded by FOFI-UAQ 2018.

Appendix A. Supplementary data

Supplementary data to this article can be found online at https://doi.org/10.1016/j.foodchem.2021.130528.

References

Agudelo, C. D., Luzardo-Ocampo, I., Campos-Vega, R., Loarca-Piña, G., & Maldonado-Celis, M. E. (2018). Bioaccessibility during *in vitro* digestion and antiproliferative effect of bioactive compounds from Andean berry (*Vaccinium meridionale* Swartz) juice. *Journal of Agricultural and Food Chemistry, 66*(28), 7358–7366. https://doi.org/10.1021/acs.jafc.8b0160410.1021/acs.jafc.8b01604.s001.

Alañón, M. E., Palomo, I., Rodríguez, L., Fuentes, E., Arráez-Román, D., & Segura-Carretero, A. (2019). Antiplatelet activity of natural bioactive extracts from mango (*Mangifera indica* L.) and its by-products. *Antioxidants, 8*(11), 517. https://doi.org/10.1016/j.foodres.2012.08.004.

Anaya-Loyola, M. A., García-Marín, G., García-Gutiérrez, D. G., Castaño-Tostado, E., Reynoso-Camacho, R., López-Ramos, J. E., … Pérez-Ramírez, I. F. (2020). A mango (*Mangifera indica* L.) juice by-product reduces gastrointestinal and upper respiratory tract infection symptoms in children. *Food Research International, 109492*. https://doi.org/10.1016/j.foodres.2020.109492.

Barnes, R. C., Krenek, K. A., Meibohm, B., Mertens-Talcott, S. U., & Talcott, S. T. (2016). Urinary metabolites from mango (*Mangifera indica* L. cv. Keitt) galloyl derivatives and *in vitro* hydrolysis of gallotannins in physiological conditions. *Molecular Nutrition & Food Research, 60*(3), 542–550. https://doi.org/10.1002/mnfr.201500706.

Bertha, C.-T., Alberto, S.-B., Tovar, J., Sáyago-Ayerdi, S. G., & Zamora-Gasga, V. M. (2019). *In vitro* gastrointestinal digestion of mango by-product snacks: Potential absorption of polyphenols and antioxidant capacity. *International Journal of Food Science & Technology, 54*(11), 3091–3098. https://doi.org/10.1111/ijfs.v54.1110.1111/ijfs.14224.

Burton-Freeman, B. M., Sandhu, A. K., & Edirisinghe, I. (2017). Mangos and their bioactive components: Adding variety to the fruit plate for health. *Food & Function, 8*(9), 3010–3032. https://doi.org/10.1039/C7FO00190H.

Cai, K., Hagerman, A. E., Minto, R. E., & Bennick, A. (2006). Decreased polyphenol transport across cultured intestinal cells by a salivary proline-rich protein. *Biochemical Pharmacology, 71*(11), 1570–1580. https://doi.org/10.1016/j.bcp.2006.02.013.

Campos-Vega, R., Vázquez-Sánchez, K., López-Barrera, D., Loarca-Piña, G., Mendoza-Díaz, S., & Oomah, B. D. (2015). Simulated gastrointestinal digestion and *in vitro* colonic fermentation of spent coffee (*Coffea arabica* L.): Bioaccessibility and intestinal permeability. *Food Research International, 77*, 156–161. https://doi.org/10.1016/j.foodres.2015.07.024.

Cheema, S., & Sommerhalter, M. (2015). Characterization of polyphenol oxidase activity in Ataulfo mango. *Food Chemistry, 171*, 382–387. https://doi.org/10.1016/j.foodchem.2014.09.011.

Clifford, M. N., Johnston, K. L., Knight, S., & Kuhnert, N. (2003). Hierarchical scheme for LC-MS identification of chlorogenic acids. *Journal of Agricultural and Food Chemistry, 51*(10), 2900–2911. https://doi.org/10.1021/jf026187q.

da Silva Haas, I. C., Toaldo, I. M., Gomes, T. M., Luna, A. S., de Gois, J. S., & Bordignon-Luiz, M. T. (2019). Polyphenolic profile, macro-and microelements in bioaccessible fractions of grape juice sediment using *in vitro* gastrointestinal simulation. *Food Bioscience, 27*, 66–74. https://doi.org/10.1016/j.fbio.2018.11.002.

Dahlgren, D., & Lennernäs, H. (2019). Intestinal permeability and drug absorption: Predictive experimental, computational and *in vivo* approaches. *Pharmaceutics, 11*(8), 411. https://doi.org/10.3390/pharmaceutics11080411.

Dars, A. G., Hu, K., Liu, Q., Abbas, A., Xie, B., & Sun, Z. (2019). Effect of thermo-sonication and ultra-high pressure on the quality and phenolic profile of mango juice. *Foods, 8*(8), 298. https://doi.org/10.3390/foods8080298.

Domínguez-Ávila, J. A., Wall-Medrano, A., Velderrain-Rodríguez, G. R., Chen, C.-Y.-O., Salazar-López, N. J., Robles-Sánchez, M., & González-Aguilar, G. A. (2017). Gastrointestinal interactions, absorption, splanchnic metabolism and pharmacokinetics of orally ingested phenolic compounds. *Food & Function, 8*(1), 15–38. https://doi.org/10.1039/C6FO01475E.

Dorta, E., González, M., Lobo, M. G., Sánchez-Moreno, C., & de Ancos, B. (2014). Screening of phenolic compounds in by-product extracts from mangoes (*Mangifera indica* L.) by HPLC-ESI-QTOF-MS and multivariate analysis for use as a food ingredient. *Food Research International, 57*, 51–60. https://doi.org/10.1016/j.foodres.2014.01.012.

Ehianeta, T. S., Laval, S., & Yu, B. (2016). Bio-and chemical syntheses of mangiferin and congeners. *Biofactors, 42*(5), 445–458. https://doi.org/10.1002/biof.1279.

Hernández-Maldonado, L. M., Blancas-Benítez, F. J., Zamora-Gasga, V. M., Cárdenas-Castro, A. P., Tovar, J., & Sáyago-Ayerdi, S. G. (2019). *In vitro* gastrointestinal digestion and colonic fermentation of high dietary fiber and antioxidant-rich mango (*Mangifera indica* L.) "Ataulfo"-based fruit bars. *Nutrients, 11*(7), 1564. https://doi.org/10.3390/nu11071564.

Herrera-Cazares, L. A., Hernández-Navarro, F., Ramírez-Jiménez, A. K., Campos-Vega, R., Reyes-Vega, M.d.l. L., Loarca-Piña, G., … Gaytán-Martínez, M. (2017). Mango-bagasse functional-confectionery: Vehicle for enhancing bioaccessibility and permeability of phenolic compounds. *Food & Function, 8*(11), 3906–3916. https://doi.org/10.1039/C7FO00873B.

Herrera-Cazares, L. A., Ramírez-Jiménez, A. K., Wall-Medrano, A., Campos-Vega, R., Loarca-Piña, G., Reyes-Vega, M. L., … Gaytán-Martínez, M. (2019). Untargeted metabolomic evaluation of mango bagasse and mango bagasse-based confection under *in vitro* simulated colonic fermentation. *Journal of Functional Foods, 54*, 271–280. https://doi.org/10.1016/j.jff.2019.01.032.

Jhaumeer Laulloo, S., Bhowon, M. G., Soyfoo, S., & Chua, L. S. (2018). Nutritional and biological evaluation of leaves of *Mangifera indica* from Mauritius. *Journal of Chemistry, 2018*, 1–9. https://doi.org/10.1155/2018/6869294.

Jiamboonsri, P., Pithayanukul, P., Bavovada, R., Leanpolchareanchai, J., Yin, T., Gao, S., & Hu, M. (2015). Factors influencing oral bioavailability of Thai mango seed kernel extract and its key phenolic principles. *Molecules, 20*(12), 21254–21273. https://doi.org/10.3390/molecules201219759.

Kiss, A. K., & Piwowarski, J. P. (2019). Ellagitannins, gallotannins and their metabolites-The contribution to the anti-inflammatory effect of food products and medicinal plants. *Current Medicinal Chemistry, 25*(37), 4946–4967. https://doi.org/10.2174/0929867323666160919111559.

Krook, M. A., & Hagerman, A. E. (2012). Stability of polyphenols epigallocatechin gallate and pentagalloyl glucose in a simulated digestive system. *Food Research International, 49*(1), 112–116. https://doi.org/10.1016/j.foodres.2012.08.004.

Lizárraga-Velázquez, C. E., Hernández, C., González-Aguilar, G. A., & Heredia, J. B. (2018). Effect of hydrophilic and lipophilic antioxidants from mango peel (*Mangifera indica* L. cv. Ataulfo) on lipid peroxidation in fish oil. *CyTA - Journal of Food, 16*(1), 1095–1101. https://doi.org/10.1080/19476337.2018.1513425.

Lucas-González, R., Viuda-Martos, M., Álvarez, J. A. P., & Fernández-López, J. (2018). Changes in bioaccessibility, polyphenol profile and antioxidant potential of flours obtained from persimmon fruit (*Diospyros kaki*) co-products during *in vitro* gastrointestinal digestion. *Food Chemistry, 256*, 252–258. https://doi.org/10.1016/j.foodchem.2018.02.128.

Luzardo-Ocampo, I., Ramírez-Jiménez, A. K., Cabrera-Ramírez, Á. H., Rodríguez-Castillo, N., Campos-Vega, R., Loarca-Piña, G., & Gaytán-Martínez, M. (2020). Impact of cooking and nixtamalization on the bioaccessibility and antioxidant capacity of phenolic compounds from two sorghum varieties. *Food Chemistry, 309*, 125684. https://doi.org/10.1016/j.foodchem.2019.125684.

Pacheco-Ordaz, R., Antunes-Ricardo, M., Gutiérrez-Uribe, J., & González-Aguilar, G. (2018). Intestinal permeability and cellular antioxidant activity of phenolic compounds from mango (*Mangifera indica* cv. Ataulfo) peels. *International Journal of Molecular Sciences, 19*(2), 514. https://doi.org/10.3390/ijms19020514.

Ramírez-Maganda, J., Blancas-Benítez, F. J., Zamora-Gasga, V. M., García-Magaña, M. d. L., Bello-Pérez, L. A., Tovar, J., & Sáyago-Ayerdi, S. G. (2015). Nutritional properties and phenolic content of a bakery product substituted with a mango (*Mangifera indica*) 'Ataulfo' processing by-product. *Food Research International, 73*, 117–123. https://doi.org/10.1016/j.foodres.2015.03.004.

Reis, A., Perez-Gregorio, R., Mateus, N., & de Freitas, V. (2020). Interactions of dietary polyphenols with epithelial lipids: Advances from membrane and cell models in the study of polyphenol absorption, transport and delivery to the epithelium. *Critical Reviews in Food Science and Nutrition, 1–24*. https://doi.org/10.1080/10408398.2020.1791794.

Sáyago-Ayerdi, S. G., Moreno-Hernández, C. L., Montalvo-González, E., García-Magaña, M. L., Mata-Montes de Oca, M., Torres, J. L., & Pérez-Jiménez, J. (2013). Mexican 'Ataulfo' mango (*Mangifera indica* L) as a source of hydrolyzable tannins. Analysis by MALDI-TOF/TOF MS. *Food Research International, 51*(1), 188–194. https://doi.org/10.1016/j.foodres.2012.11.034.

Vazquez-Olivo, G., Antunes-Ricardo, M., Gutiérrez-Uribe, J. A., Osuna-Enciso, T., León-Félix, J., & Heredia, J. B. (2019). Cellular antioxidant activity and *in vitro* intestinal permeability of phenolic compounds from four varieties of mango bark (*Mangifera indica* L.). *Journal of the Science of Food and Agriculture, 99*(7), 3481–3489. https://doi.org/10.1002/jsfa.2019.99.issue-710.1002/jsfa.9567.

Wall-Medrano, A., Olivas-Aguirre, F. J., Ayala-Zavala, J. F., Domínguez-Avila, J. A., Gonzalez-Aguilar, G. A., Herrera-Cazares, L. A., & Gaytan-Martinez, M. (2020). Health Benefits of Mango By-products. In R. Campos-Vega, B. D. Oomah, & H. A. Vergara-Castañeda (Eds.), Food Wastes and By-products: Nutraceutical and health potential; John Wiley & Sons Ltd. ISBN 978-1-119-53410-5 (First, pp. 159–191). Doi: 10.1002/9781119534167.ch6.

Zepeda-Ruiz, G. C., Domínguez-Avila, J. A., Ayala-Zavala, F., Robles-Sánchez, M., Salazar-López, N. J., López-Díaz, J. A., & González-Aguilar, G. (2020). Supplementing corn chips with mango cv. "Ataulfo" peel improves their sensory acceptability and phenolic profile, and decreases *in vitro* dialyzed glucose. *Journal of Food Processing and Preservation, 44*(12), Article e14954. https://doi.org/10.1111/jfpp.14954.

Food Chemistry

Supplementary Electronic Material

Gastrointestinal metabolism of monomeric and polymeric polyphenols from mango (*Mangifera indica* L. cv. Ataulfo) bagasse under simulated conditions

Luz Abril Herrera-Cazares [a**], Aurea K. Ramírez-Jiménez [b**], Ivan Luzardo-Ocampo [a], Marilena Antunes-Ricardo [b], Guadalupe Loarca-Piña [a], Abraham Wall-Medrano [c], Marcela Gaytán-Martínez [a*]

[a] Research and Graduate Program in Food Science, School of Chemistry, Universidad Autónoma de Querétaro, Cerro de las Campanas S/N. Col. Centro, 76010 Santiago de Querétaro, Qro., México

[b] Tecnológico de Monterrey, School of Engineering and Science, Av. Eugenio Garza Sada 2501 Sur, C.P. 64849, Monterrey, N.L., México

[c] Instituto de Ciencias Biomédicas, Universidad Autónoma de Ciudad Juárez, Anillo Envolvente del PRONAF y Estocolmo s/n, 32310 Ciudad Juárez, Chihuahua, México.

** These authors equally contributed to this manuscript.

*Corresponding author: Tel. /fax: +52 442 192 1307, E-mail address: marcelagaytanm@yahoo.com.mx (Gaytán-Martínez M.)

Supplementary Fig. S1. AIF and BIF fractions from the simulated gastrointestinal digestion (SGD).

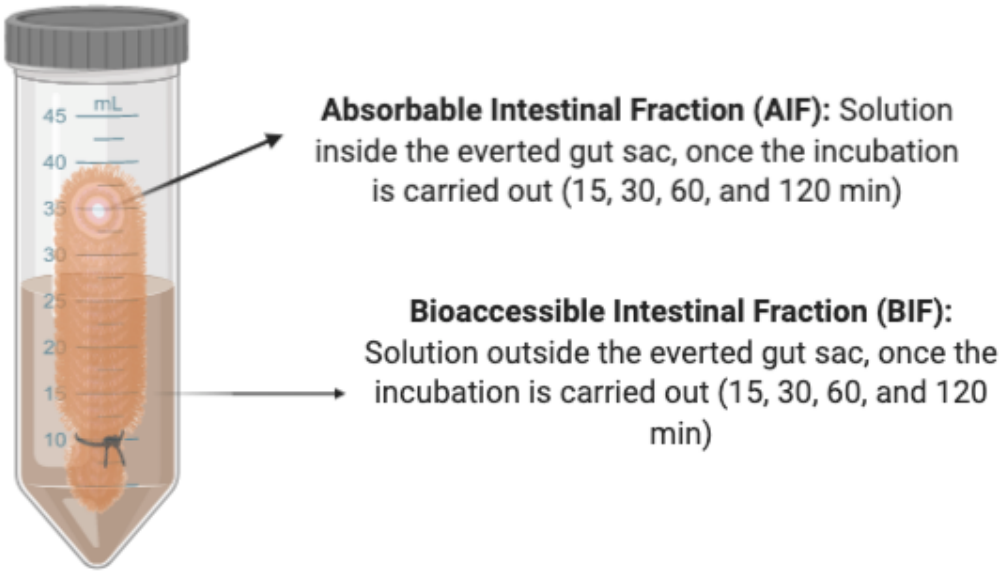

The graphic was done with Biorender.com software.

Supplementary Fig. S2. Mass spectra of the identified phenolic compounds by LC/MS-ESI-TOF.

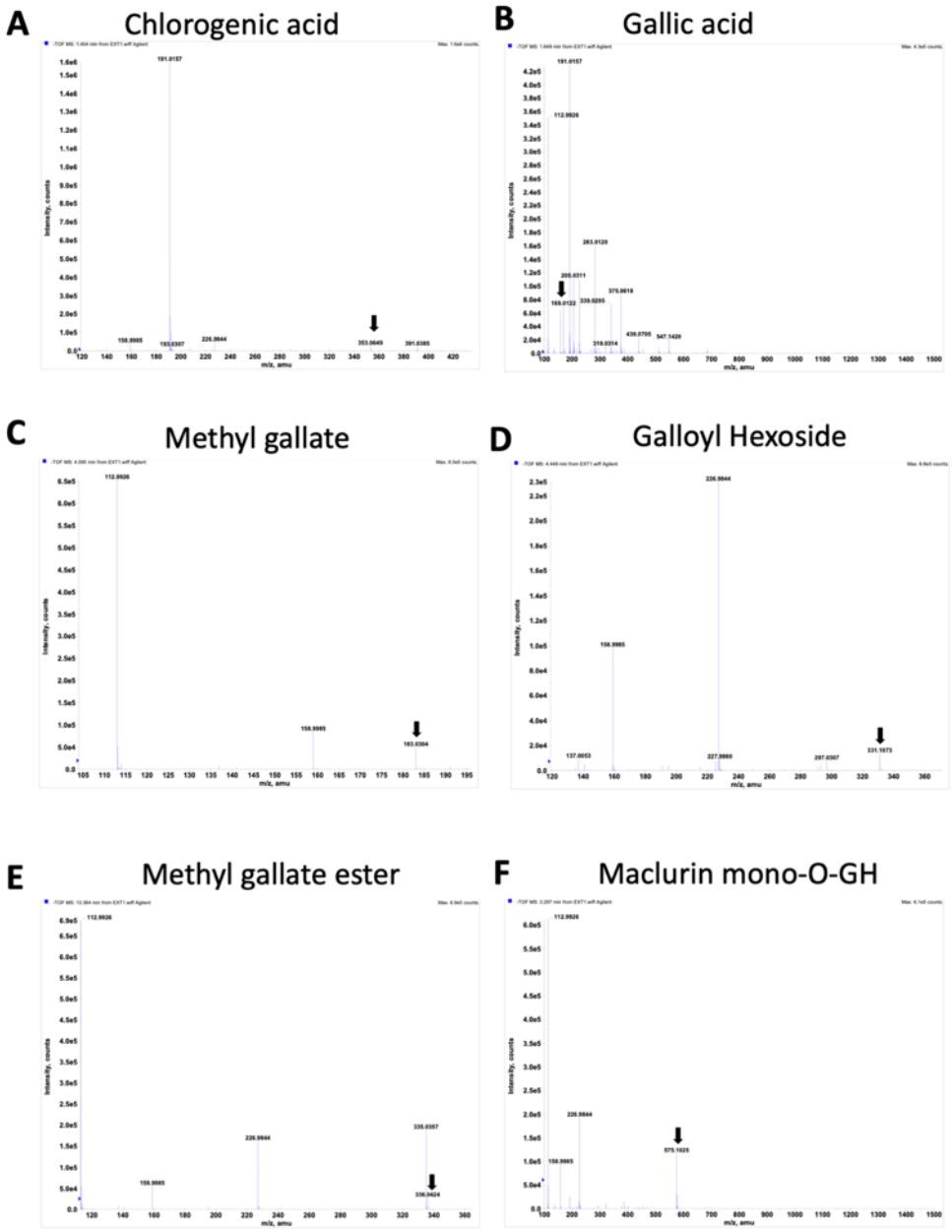

G

Maclurin-di-O-GH

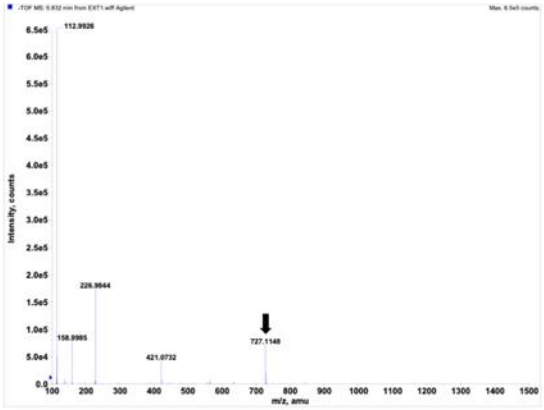

H

Mangiferin

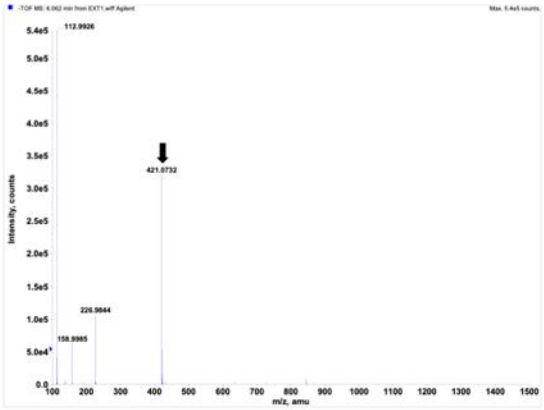

I

Isomangiferin

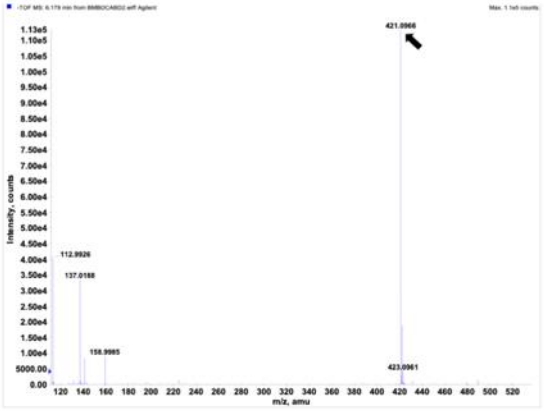

J

Homomangiferin

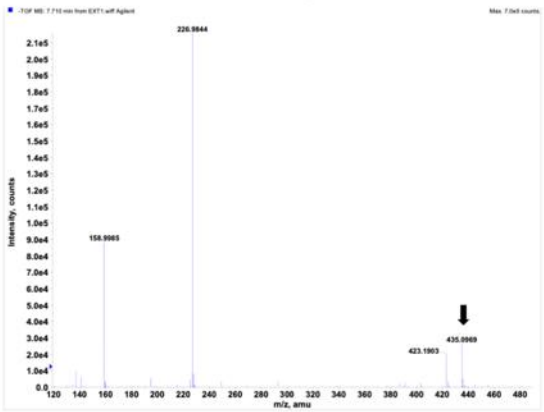

K

Digallic acid

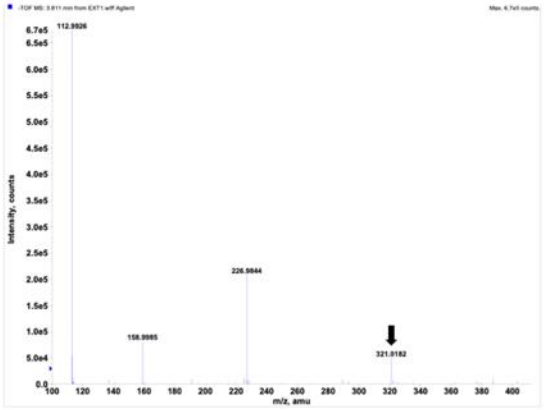

L

Penta-O-galloyl-hexoside

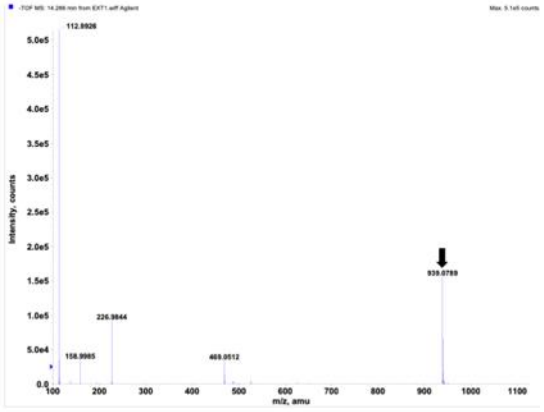

M Hexa-O-galloyl hexoside

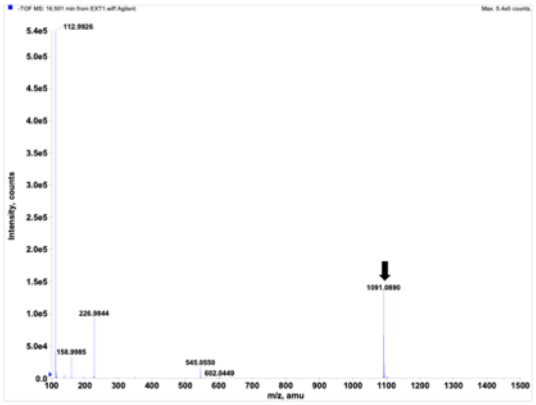

N Hepta-O-galloyl hexoside

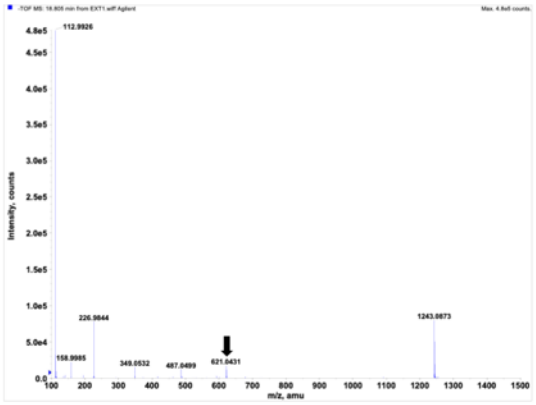

O Octa-O-galloyl hexoside

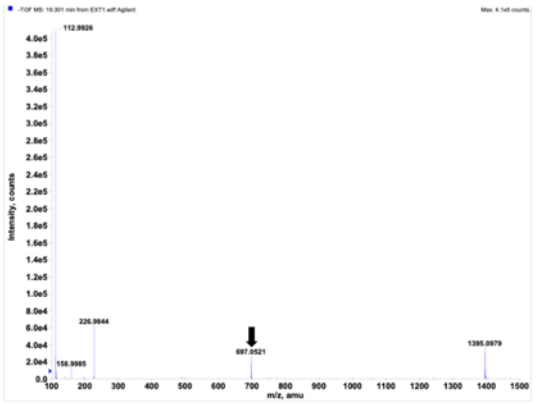

P Quercetin

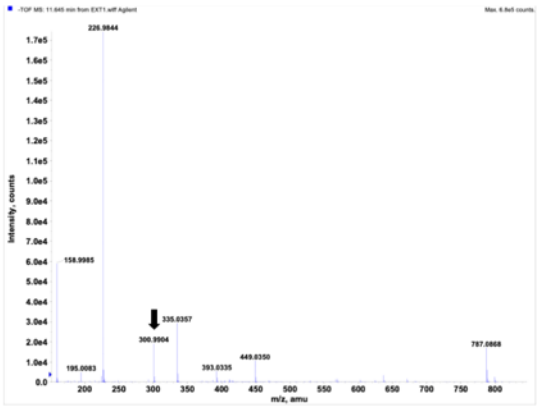

Q Quercetin Hexoside

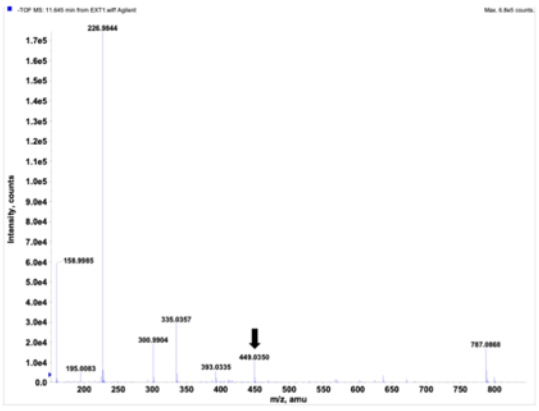

Supplementary Fig. S3. Principal component analysis (PCA) of MB polyphenols and antioxidant capacity during SGD. **(A)** Participation (%) of each component; (**B**) Eigenvalues from the first 3 components.

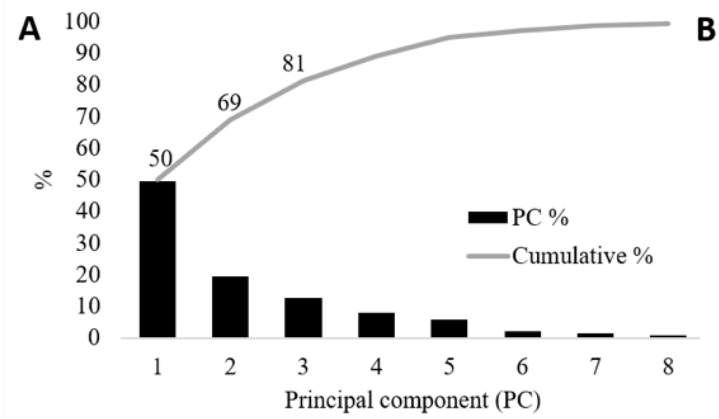

B

Variable	PC1	PC2	PC3
Phenolic acids			
CA	-0.082	0.253	-0.420
GA	0.062	0.439	0.013
GG	0.288	0.099	0.089
MG	0.310	-0.059	-0.063
MGE	0.279	0.024	-0.208
Gallotannins			
DA	-0.038	-0.352	0.337
3GG	-0.105	-0.127	-0.096
5GG	0.307	-0.084	-0.099
6GG	0.312	-0.049	-0.060
7GG	0.306	0.005	0.025
8GG	0.303	-0.095	-0.112
Benzophenones			
MGG	0.206	0.317	0.229
MDG	0.012	0.096	-0.308
Xanthones			
HMan	0.072	0.069	0.472
Man	0.232	0.300	0.105
Flavonoids			
Quer	0.252	-0.154	-0.056
QuerG	0.287	0.220	-0.169
Antioxidant capacity			
DPPH	0.226	-0.325	0.077
ABTS	0.204	-0.362	0.067

Absorbable (AIF) and bioaccessible (BIF) intestinal fractions, bounded polyphenol (BPC), chlorogenic acid (CA), free polyphenol (FPC), gallic acid (GA) equivalents (GAE), galloyl glucoside (GG), homomangiferin (HMan), mangiferin (Man) equivalents (ManE), methyl gallate (MG), methyl gallate ester (MGE), polyphenol (PC), quercetin (Quer), equivalents (QE) and glucoside (QuerG), simulated gastrointestinal digestion (SGD).

Supplementary Table S1. (A) Physicochemical characteristics of the mango bagasse; **(B)** Physicochemical characterization of mango pulp.

(A)

Parameter		Value
Physicochemical characterization		
Color (CIEL*a*b* space)	L*	73.24 ± 0.30
	a*	11.44 ± 0.10
	b*	45.16 ± 0.83
Water absorption index (g gel/g MB flour)		12.98 ± 0.16
Water solubility index (%)		44.43 ± 1.86
Proximal Composition (%)[1]		
Protein		0.98 ± 0.58
Lipids		1.20 ± 0.17
Ash		2.74 ± 0.12
Moisture		60.52 ± 1.16
Carbohydrates		34.56 ± 2.53
Total dietary fiber		11.45 ± 0.67
Soluble dietary fiber		6.71 ± 0.39
Insoluble dietary fiber		4.72 ± 0.28

[1] (Herrera-Cazares et al., 2017).

(B)

Parameter		Value
Physicochemical characterization[2]		
Color (CIEL*a*b* space)	L*	49.90 ± 1.60
	a*	0.84 ± 0.20
	b*	30.70 ± 2.30
	hº	89.20 ± 1.70
pH		3.51 ± 0.07
TSS (º Brix)		17.70 ± 0.60
TA (%)		0.81 ± 0.17
Water solubility index (%)		44.43 ± 1.86
Proximal composition (%)[2]		
Total dietary fiber		12.65 ± 0.51
Soluble dietary fiber		3.92 ± 0.38
Insoluble dietary fiber		8.73 ± 0.89

[2] (Barrón-García et al., 2021).

Supplementary Table S2. Content of MB polyphenols (PC) during SGD: phenolic acids, flavonoids and xanthones

PC	FPC	BPC	Oral	Gastric	AIF (min)				BIF (min)			
					15	30	60	120	15	30	60	120
Phenolic acids (280 nm, mg GAE/g sample)												
CA	133.5 ± 14.3 ^{CDbc}	--	144.6 ± 15.8 ^{CDb}	222.4 ± 56.6 ^{BCbc}	655.2 ± 16.2 ^{Aa}	173.5 ± 18.7 ^{BCDa}	209.9 ± 22.4 ^{BCa}	257.0 ± 32.6 ^{BCa}	293.2 ± 57.1 ^{BCa}	285.9 ± 88.7 ^{BCa}	252.9 ± 12.3 ^{BCa}	346.3 ± 22.0 ^{Ba}
GA	193.9 ± 10.4 ^{ABCDbc}	--	285.4 ± 35.3 ^{ABa}	325.9 ± 9.08 ^{ABa}	166.7 ± 86.0 ^{ABCDb}	50.7 ± 8.4 ^{CDb}	135.7 ± 33.2 ^{BCDa}	194.5 ± 47.6 ^{ABCDa}	261.2 ± 66.4 ^{ABCa}	315.7 ± 62.7 ^{ABa}	177.2 ± 66.7 ^{ABCDab}	347.7 ± 13.3 ^{Aa}
GH	18.2 ± 0.2 ^{Ac}	--	--	15.9 ± 3.0 ^{Ae}	--	--	--	--	7.5 ± 2.2 ^{Bb}	--	--	--
MG	34.4 ± 11.6 ^{Ac}	--	--	11.5 ± 1.9 ^{Bc}	--	--	--	--	--	--	--	--
MHE	45.9 ± 12.6 ^{Ac}	--	--	15.7 ± 3.9 ^{Be}	8.1 ± 1.5 ^{Bc}	9.8 ± 0.4 ^{Bbc}	--	3.9 ± 0.6 ^{Bb}	11.4 ± 2.4 ^{Bb}	12.8 ± 1.0 ^{Bc}	18.4 ± 6.7 ^{Bcd}	15.8 ± 4.2 ^{Bc}
Flavonoids (365 nm, µg QE/g of sample)												
Quer	13.0 ± 0.5 ^{Ac}	0.5 ± 0.02 ^{Bb}	--	--	--	--	--	--	--	--	--	--
QuerH	61.4 ± 1.3 ^{Ac}	5.0 ± 0.3 ^{Deb}	32.0 ± 2.6 ^{BCc}	44.5 ± 4.7 ^{ABe}	23.9 ± 4.8 ^{BCDEc}	28.8 ± 6.2 ^{BCDbc}	--	9.9 ± 1.3 ^{DEa}	40.7 ± 8.0 ^{ABb}	33.5 ± 7.1 ^{BCbc}	31.2 ± 4.9 ^{BCcd}	19.4 ± 1.5 ^{CDEc}
Xanthones (360 nm, µg ManE/ g of sample)												
HMan	--	4.3 ± 1.6 ^{Bb}	--	9.2±0.7 ^{Ae}	--	--	--	--	--	--	--	--
Man	284.8 ± 6.6 ^{Abc}	1.9 ± 0.7 ^{Db}	162.9 ± 8.9 ^{Bb}	290.5 ± 18.5 ^{Aab}	25.0 ± 1.4 ^{CDc}	33.5 ± 6.9 ^{CDbc}	31.3 ± 5.0 ^{CDb}	45.4 ± 12.8 ^{CDb}	195.0 ± 52.0 ^{ABa}	212.9 ± 31.0 ^{ABa}	128.7 ± 21.9 ^{BCbc}	161.2 ± 20.7 ^{Bb}
IMan	--	1.7 ± 0.5 ^{Bb}	11.1 ± 0.8 ^{Ac}	12.4 ± 3.1 ^{Ae}	--	--	--	--	--	--	--	--

Results are expressed as the average ± SD from three independent randomized experiments by triplicates. Upper-case letters in a same row indicate significant differences ($p<0.05$) by Tukey-Kramer's test between digestion stages for a compound while lower-case letters indicate significant differences between all compounds for a same digestion step. Absorbable (AIF) and bioaccessible (BIF) intestinal fractions, bound polyphenols (BPC), chlorogenic acid (CA), free polyphenols (FPC), gallic acid (GA) equivalents (GAE), galloyl glucoside (GG), homomangiferin (HMan), mangiferin (Man) equivalents

(ManE), methyl gallate (MG), methyl gallate ester (MGE), polyphenol (PC), quercetin (Quer), equivalents (QE) and hexoside (QuerH), simulated gastrointestinal digestion (SGD), not detected (--).

Supplementary Table S3. Content of MB polyphenols (PC) during SGD: Benzophenones and gallotannins

PC	FPC	BPC	Oral	Gastric	AIF (min)				BIF (min)			
					15	30	60	120	15	30	60	120
Benzophenones (280 nm, mg GAE/g sample)												
MGH	19.7 ± 0.4 ^{ABCDc}	--	19.5 ± 2.3 ^{ABCc}	27.0 ± 1.2 ^{Ae}	--	--	--	--	19.7 ± 0.1 ^{ABb}	9.4 ± 5.7 ^{BCDEc}	9.7 ± 2.4 ^{CDEd}	9.3 ± 3.3 ^{DEc}
MDH	28.7 ± 2.0 ^{BCc}	--	8.3 ± 0.7 ^{DEc}	30.0 ± 2.5 ^{Be}	148.3 ± 10.1 ^{Ab}	4.2 ± 1.0 ^{Dec}	--	5.3 ± 0.5 ^{DEb}	17.0 ± 1.5 ^{CDb}	--	--	4.5 ± 0.8 ^{DEc}
Gallotannins (280 nm, mg GAE/g sample)												
DA	n.d.	246.6 ± 18.7 ^{Aa}	--	--	--	--	--	2.9 ± 0.96 ^{Bb}	6.2 ± 0.8 ^{Bb}	8.2 ± 3.3 ^{Bc}	5.9 ± 2.4 ^{Bd}	7.3 ± 3.0 ^{Bc}
3G	17.1 ± 0.8 ^{Cc}	12.7 ± 0.7 ^{Cb}	16.7 ± 2.0 ^{Cc}	36.4 ± 4.0 ^{Ce}	5.0 ± 0.6 ^{Cc}	185.9 ± 14.5 ^{Aa}	125.3 ± 5.4 ^{Ba}	171.1 ± 14.1 ^{Aa}	24.1 ± 3.8 ^{Cb}	18.0 ± 7.7 ^{Cc}	8.1 ± 1.0 ^{Cd}	21.5 ± 2.5 ^{Cc}
5G	328.5 ± 21.2 ^{Abc}	--	--	76.9 ± 11.9 ^{Bde}	--	--	--	--	--	--	--	--
6G	455.0 ± 10.3 ^{Aab}	--	7.4 ± 2.1 ^{Cc}	157.7 ± 25.5 ^{Bcd}	--	--	--	3.4 ± 0.2 ^{Cb}	8.5 ± 1.4 ^{Cb}	10.7 ± 2.3 ^{Cc}	5.7 ± 1.2 ^{Cd}	6.4 ± 1.2 ^{Cc}
7G	338.6 ± 74.0 ^{Abc}	--	13.7 ± 2.4 ^{Cc}	201.9 ± 28.6 ^{Bbc}	3.8 ± 0.9 ^{Cc}	3.7 ± 0.5 ^{Cc}	6.5 ± 1.4 ^{Cb}	--	--	--	--	--
8G	704.7 ± 23.4 ^{Aa}	--	--	145.0 ± 18.3 ^{BCe}	--	--	--	54.2 ± 11.0 ^{Bb}	--	--	--	--

Results are expressed as the average ± SD from three independent randomized experiments by triplicates. Upper-case letters in a same row indicate significant differences ($p<0.05$) by Tukey-Kramer's test between digestion stages for a compound while lower-case letters indicate significant differences between all compounds for a same digestion step. Tri- (3G), penta- (5G), hexa- (6G), hepta- (7G) and octa (8G)-*O*-galloyl hexosides, absorbable (AIF) and bioaccessible (BIF) intestinal fractions, bounded polyphenol (BPC), di-gallic acid (DA), free polyphenol (FPC), gallic acid equivalents (GAE), maclurin-mono (MGH) and di (MDH)-galloyl hexoside, polyphenol (PC), simulated gastrointestinal digestion (SGD), not detected (--).

Supplementary Table S4. Apparent permeability (*Papp*) of MB polyphenols: Kinetic data

PC	P_{app} A to B					P_{app} B to A				
	X^3	X^2	X	b	R^2	X^3	X^2	X	b	R^2
Dynamic permeants										
CA		0.003	-0.52	22.4	0.94	-4.0E-04	0.092	-5.51	96.4	0.99
GA		0.002	-0.34	14.9	0.98	8.0E-05	0.017	-1.00	17.1	0.99
Man		0.001	-0.18	8.5	0.99	-1.0E-05	0.002	-0.13	2.4	0.99
MGE		0.001	-0.22	11.5	0.89		0.001	-0.22	8.2	0.93
QuerH		0.002	-0.37	15.8	0.90		0.001	-0.23	8.5	0.93
Apical (A) prone										
MDH	--	--	--	--	--	-8.0E-04	0.160	-9.607	165.320	0.99
3G		0.006	-0.11	5.1	0.97	2.0E-04	-0.045	-2.53	-27.0	0.99
7G	--	--	--	--	--		4.0E-05	-0.005	0.250	0.84
Basolateral (B) prone										
DA	4.0E-05	0.008	-0.51	9.0	0.99	--	--	--	--	--
MGH		0.002	-0.29	11.0	0.86	--	--	--	--	--
6G		0.000	-0.02	0.7	0.98	--	--	--	--	--

[1] Goodness of fit (GOF) linear regression. See **Table 1** for compound codes. Not calculated due to lack of enough time-trend data (--), absorbable (AIF) and bioaccessible (BIF) intestinal fractions.

References

Barrón-García, O. Y., Gaytán-Martínez, M., Ramírez-Jiménez, A. K., Luzardo-Ocampo, I., Velázquez, G., & Morales-Sánchez, E. (2021). Physicochemical characterization and polyphenol oxidase inactivation of Ataulfo mango pulp pasteurized by conventional and ohmic heating processes. *LWT, 143*, 111113. https://doi.org/10.1016/j.lwt.2021.111113

Herrera-Cazares, L. A., Hernández-Navarro, F., Ramírez-Jiménez, A. K., Campos-Vega, R., Reyes-Vega, Maria de la Luz, Loarca-Piña, G., Wall-Medrano, A., Gaytán-Martínez, M. (2017). Mango-bagasse functional confectionery: vehicle for enhancing bioaccessibility and permeability of phenolic compounds. *Food and Function, 8*(11), 3906-3916. https://doi.org/10.1039/C7FO00873B